Summer 9-20-2018

Removal Efficiencies, Uptake Mechanisms and Competitive Effects of Copper and Zinc in Various Stormwater Filter Media

Emily Heleva-Ponaski
Portland State University

Removal Efficiencies, Uptake Mechanisms and Competitive Effects of Copper and Zinc in Various Stormwater Filter Media

by

Emily Heleva-Ponaski

A thesis submitted in partial fulfillment of the
requirements for the degree of

Master of Science
in
Civil and Environmental Engineering

Thesis Committee:
Gwynn Johnson, Chair
William Fish
James Pankow

Portland State University
2018

ABSTRACT

Polluted stormwater, if not treated, can compromise water quality throughout our hydrologic cycle, adversely affecting aquatic ecosystems. Common stormwater pollutants, copper and zinc, have been identified as primary toxicants in multiple freshwater and marine environments. For small-scale generators, stormwater management can be cumbersome and implementation of common BMPs impractical thus catch basins are popular though not the most environmentally conscious and sustainable option. This study aims to characterize the potential of a mobile media filter operation for the treatment and on-site recycling of catch basin stormwater. The removal capacities of various commercially available filter media (e.g. a common perlite; Earthlite™, a medium largely composed of biochars; and Filter33™, a proprietary porous medium) were measured using binary injection solutions modeled after local catch basin stormwater characteristics. The results of filtration experiments, rapid small-scale column tests (RSSCTs), indicate that the transport of metals in Perlite is primarily impacted by nonspecific sorption whereas in Earthlite™ and Filter33™ both nonspecific and specific sorption are present. For all media and experimentation, there was a consistent preferential uptake of copper such that copper displayed delayed arrival and/or greater removal than zinc. Moreover, the observed snow plow effects and concentration plateaus in Earthlite™ and Filter33™ RSSCTs suggest rate limited ion exchange and specific sorption in addition to ion competition. Earthlite™ exhibited an approach velocity dependent removal

efficiency in the RSSCTs and pseudo second order uptake behavior for zinc in kinetic batch experiments. At the lab scale equivalent of the proposed field scale flow rate, Filter33™ displayed the greatest average zinc removal of 8.6 mg/g. In all, this research indicates that test parameters (i.e. pH, competitive ions solutions, empty bed contact time, flow rate) based on the natural environment and field scale operation can greatly impact removal efficiency in filter media.

TABLE OF CONTENTS

LIST OF TABLES

LIST OF FIGURES

1.0 INTRODUCTION

In natural environments, stormwater is part of the water cycle, thus after a storm event, runoff water often rejoins the surrounding surface and groundwater systems. Unfortunately, in urban environments, this hydrologic flow component, either as interception, baseflow, interflow, or even infiltration, can be disrupted by impervious surfaces creating stormwater runoff. In general, stormwater runoff is commonly considered a pollutant source as overland water flow tends to gather oils, chemicals, heavy metals, and sediment from a variety of surfaces (e.g. roads, roofs). Consequently, this polluted stormwater, if not treated, can compromise water quality throughout our hydrologic cycle (USEPA, 2018b).

To address this problem, the Clean Water Act (CWA) was established in 1972 to protect surface water systems from pollution. In this act, stormwater runoff pollution is separated into two categories: nonpoint source and point source. Nonpoint source runoff pollution in an urban environment may come from streets, parks, and roofs, and is generally defined as runoff pollution without a discrete point source. Unfortunately, nonpoint source pollution is the “leading remaining cause of water quality problems” around the world (USEPA, 2017).

Point source pollution, as defined by the CWA, is “any discernible, confined and discrete conveyance…from which pollutants are or may be discharged” (USEPA, 2017). To regulate this type of pollution the United States Environmental Protection Agency (USEPA) through the CWA authorizes states to permit alternatives to stormwater management under the National Pollutant

Discharge Elimination System (NPDES) program (USEPA, 2018b). Under this program, states issue, regulate and enforce NPDES permits, while the USEPA maintains the right to oversee any and all operations. In general, NPDES permits protect surface water quality by regulating the release of pollution (e.g. heavy metals, oils and solids) from a point source to receiving surface water systems. In the United States, typical point sources requiring NPDES stormwater permits are municipal separate stormwater systems (i.e. publicly-owned conveyance systems that discharge to surface waters), construction activities (e.g. ground disruption, outdoor materials and equipment storage) and industrial activities (e.g. petroleum refineries, salvage yards, transportation facilities with cleaning operations).

Heavy metals (e.g. cadmium, copper, lead and zinc), total suspended solids (TSS), oil/grease and pH are regulated under a typical NPDES stormwater permit due to their potential adverse effects on aquatic ecosystems (USEPA, 2018b). For example, the olfactory system of salmonid species can be negatively impacted by low concentrations of copper (Sandahl et al., 2007; Baldwin et al., 2011). In a Santa Monica Bay stormwater discharge study, zinc was identified as a primary toxicant of concern in fertilization tests performed with sea urchin (Bay et al., 2003). A West Los Angeles highway runoff study found copper and zinc to be the primary cause of toxicity in 90% of freshwater and marine species sampled (Kayhanian et al., 2008). Additionally, excess solids in natural waters can be harmful to aquatic life. Increased sediment loads in receiving surface

water systems related to runoff from mining and road construction have been shown to negatively impact fish, invertebrates, spawning ground and general biological activity (Brookes, 1986; Ribaudo, 1986; Bilotta and Brazier, 2008).

In urban environments, vehicles (specifically from brake pad wear, tire wear and engine oil) are sources of heavy metal pollution in stormwater such that parking lots and road surfaces tend to display higher levels of heavy metals when compared to other common urban runoff (Davis et al., 2001; Charters et al., 2016; Huber et al., 2016). Vehicle brake pads and runoff from copper roofing and gutter materials are large contributors to copper pollution in residential and industrial areas, entering stormwater runoff through dissolution (Nason et al., 2012; Charters et al., 2016). Other copper pollution sources include, for example, metal finishing, copper plating, engine oil, fertilizers, pesticides and industrial releases (Sari el at., 2007; Ghassabzadeh et al., 2010; Nason et al., 2012). Zinc pollution typically enters the urban water system through runoff from galvanized structures, roofs, building siding, parking lots and roads (Charters et al., 2016; Huber et al., 2016). Bridge deck and building siding runoff were found to be large contributors to stormwater zinc concentration due to their concrete, painted wood and galvanized components (Davis et al., 2001; Huber et al., 2016). Additionally, roofs and roads are the primary sources of suspended solids in runoff due to atmospheric deposition of sediment from industrial activities, vehicle emissions and soils onto these surfaces and the subsequent storm events that wash them off (Charters et al. 2016).

When in a stormwater stream, heavy metals can exist in two basic forms, dissolved and particulate making TSS removal an important component of a metals' removal strategy. Many have noted the toxicity of dissolved metals in their free ion form due to their ability to bind with aquatic biota and organisms, specifically copper due to its high reactivity (Nason et al., 2012; Charters et al., 2016). NPDES permits are commonly written for total metal concentrations due to metal complexation and its dependency on stormwater characteristics (i.e. hardness, pH, cation competition and organic ligand concentration) (Kinerson et al., 1996).

With increased urbanization throughout the US, there has become a need for alternatives to traditional end of the pipe approaches to stormwater treatment. Many municipalities have developed stormwater management plans to help address the obstacles and practicalities in removing pollutants from various and challenging sources as well as offering an alternative to traditional treatment through best management practices (BMPs) (USEPA, 2018b). BMPS are stormwater controls that have been identified as ways to treat stormwater at its source, thereby decreasing the load sent to a wastewater treatment plant. As a result, BMPs can reduce costs, redirect stormwater back into the natural environment and protect the environment from pollutants.

Commonly employed BMPs include biofilters, catch basins and media filters. Biofilters range from rain gardens, bioswales, ecology embankments, to retention ponds and constructed wetlands. These treatment systems aim to

capture and hold the runoff allowing for infiltration and removal of pollutants (ODEQ, 2003; BES, 2004; Soil Science Society of America, 2018). Typically, the delineation between various biofilters tends to lie in the size, construction, soil amendments and treatment areas. Catch basins and media filters basically separate the processes that a biofilter does into two distinct phases where, for example, the catch basin aims to collect and store runoff while the media filter aims to treat runoff.

A catch basin is usually a square concrete hole with a grate on top at a runoff low point, though design and construction vary by location. In some applications, catch basins are connected to the local/regional stormwater system by drains and are primarily meant to help reduce the sediment load in the runoff before feeding the stormwater into the conveyance system (Figure 1)(ODEQ, 2017). Other catch basins simply store runoff until it can be removed or treated (e.g. a pump and haul approach to stormwater management). Regardless of type, catch basins need to be maintained by cleaning and/or emptying settled solids, but the frequency depends on location and precipitation.

A media filter, or stormwater filter, contains a filter medium designed to target the primary pollutants of the source area it is treating. Stormwater flows through the media filter which in application removes or filters the pollutant, leaving treated water that then can be discharged into the environment (assuming treatment levels have met local, permitted NPDES requirements) (Barrett, 2005). This eliminates the need for removal and transportation

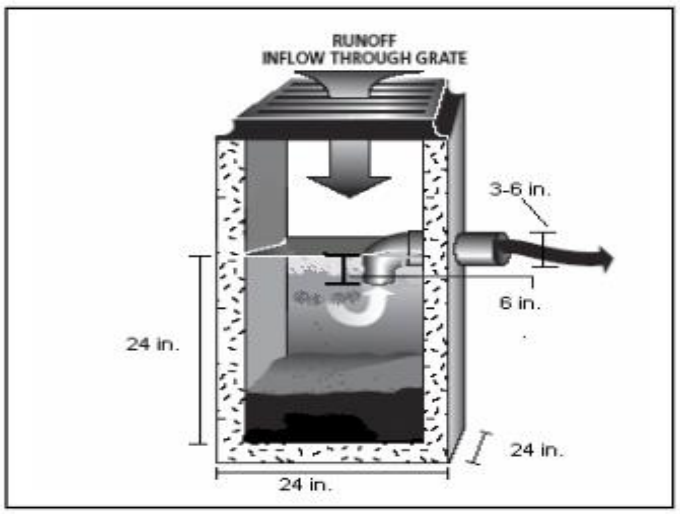

Figure 1. Standard Lynch-style catch basin with City of Portland design specifications (ODEQ, 2017).

(e.g. pump and haul) of the polluted water and while this alternative to managing stormwater carries operation and maintenance costs it is widely considered a cost-effective and sustainable option for many generators.

It is common for multiple and various generators in a similar geographical area, all held to the same total maximum daily load (TMDL) pollutant limits, to use similar BMPs (USEPA, 2018a). At the municipality or corporation level, for example, the implementation of biofilters, conveyance alteration and/or other common BPMs is typically considered practical (BES, 2016). On the other hand, on-site stormwater management plans for smaller, private businesses may need alternative solutions. Some companies can and do invest in alternatives (for example, Arbor Lodge New Seasons, Portland, OR installed a bioswale in the center of their parking lot), but space and upfront investment costs can create barriers. There appears to be a need for onsite treatment of catch basin

stormwater that does not require a large initial investment and/or costly operation/maintenance for the generator that is more environmentally conscious and sustainable than pump, haul, and treat. One alternative solution many local-scale generators find applicable, as they tend to require a small footprint, are catch basins plus media filters; two convenient BMPs used in combination. Another alternative, upcoming approach includes a “mobile” media filter facility. For example, as stormwater is collected from similar pollutant loading zones (i.e. multiple on-site catch basins), the waters could be treated by the “on-truck” media filters and recycled (assuming treatment meets local, permitted NPDES requirements) on site.

This study aims to characterize the potential of a mobile media filter operation for the treatment and recycling of stormwater. The removal capacities of various commercially available filter media (e.g. a common perlite, a medium largely composed of biochars, and a proprietary porous medium) were measured using pollutant concentrations modeled after stormwater samples collected from local catch basins. NPDES permit pollutant levels were used to help characterize filter efficiency and filter lifetime. Experiments aimed to qualify filter medium performance were conducted under pumped conditions with the overall goal of the project being to characterize cost-effective and sustainable stormwater treatment alternatives for local/small-scale generators.

2.0 BACKGROUND

2.1 Metals

Copper is a transition metal that can have variable valance which translates into multiple oxidation states, Cu(I) and Cu(II). In aqueous solutions, Cu(I) is unstable and usually deprotonates to Cu(II). Cu(II) has an incomplete set of d-shell electrons (e.g. 9 electrons in the d-shell) which means that it is "strongly influenced by its surroundings, particularly by its coordinated ligands" making it one of the most reactive divalent metals (Morel and Hering, 1993). In its free divalent ion form, Cu(II) is toxic and bioavailable making it a concern in natural water systems (Nason et al., 2012).

According to the Irving-Williams series wherein the stability of complexed multivalent ions are ranked, Mn(II) < Fe(II) < Co(II) < Ni(II) < Cu(II) > Zn(II), copper has a greater complex stability than other divalent metal ions due to its high effective nuclear charge and ligand field stabilization energy (i.e. the electrostatic interaction between the d-orbital electrons and approaching ligands) (Morel and Hering, 1993). As described by Pankow (1991) when summarizing metal/ligand complexation reactions, a larger equilibrium constant equals a more stable complex. A review of stability constants of metals with ligands commonly found in natural waters and present in aquatic organic material reveals that many of the Cu(II) constants are greater than those of Zn(II) for that same metal:ligand formation.

Zinc is a post-transition metal with one oxidation state, Zn(II), and being to the right of copper on the periodic table, it is slightly larger. In its oxidized form, zinc has a full d-orbital making it more stable than copper in the aqueous environment and, therefore, less influenced by its surroundings. As discussed in Morel and Hering (1993), Zn(II) has no ligand field stabilization energy explaining “the most important difference in the relative degree of reactivity of various metal complexes”.

2.2 Sorption Mechanisms

The uptake of fluid-phase molecules (e.g. cations in solution) by a sorbent is commonly referred to as sorption, a “lumped term” capturing multiple mechanisms responsible for those sorbate/sorbent reactions. Those reactions are defined by electromagnetic interactions of the nuclei and electrons driven by both physical and chemical processes (Muralikrishna and Manickam, 2017). Physisorption (physical sorption) is a non-specific sorption that occurs as a result of weak intermolecular forces (Van der Waals forces) that do not alter the surface of the sorbent. It is common to assume that as physical sorption is due to attractive forces and not chemical bonds, it can be reversible resulting in the release (desorption) of sorbate. Chemisorption (chemical sorption) involves the creation of chemical bonds between the sorbate (e.g. the ions in solution) and the sorbent. This interaction is specific and as such alters the charge characteristics of the sorbent usually making the process irreversible. For

example, with heavy metal ions, chemisorption with silanol and aluminol groups involves a proton exchange as the metal bonds directly to the oxygen (Harsh, 2005).

$$Al - OH + M^{2+}(aq) \leftrightarrow Al - OM^{+} + H^{+} \quad (1)$$

In the above equation, the allophane surface becomes positively charged (the charge characteristics change) and the solution becomes more acidic as a proton is exchanged.

The previously mentioned sorption mechanisms take place on the surface of the sorbent (often defined as adsorption), but at times there are more complicated mechanisms (e.g. absorption reactions) taking place beyond these surface interactions such as diffusive mass transfer which includes film diffusion, pore diffusion, intraparticle diffusion and intraorganic matter diffusion (Johnson, 2005).

2.3 Ion Exchange Reactions

Ion exchange is defined when an ion in solution and an ion associated with the sorbent exchange places, changing the solution concentration of that ionic species yet preserving the electrical neutrality of the solution (Kumar and Jain, 2013). This naturally occurring process can be enhanced using manufactured sorbents (i.e. ion exchange media and resins) that target cations, anions or both. Janvion et al. (1995) described this process using Na^{+} as the exchangeable ion in the resin:

$$2Na_r^+ + M_s^{2+} \rightleftharpoons M_r^{2+} + 2Na_s^+ \quad (2)$$

where subscripts r and s denote the ion exchange resin and solution, respectively, showing it as a reversible process.

Previous research has suggested that ion exchange is a kinetically-controlled process that can involve film and particle diffusion (Helfferich and Plesset, 1958; Selim et al., 1992). Additionally, it has been reported to work in tandem with sorption reactions and possibly controls the desorption process (Caetano et al., 2009). Vaaramaa et al. (2003) observed competitive ion displacement when evaluating organic and inorganic ion exchangers for metals removal from drinking water. For example, the researchers noted effluent concentrations of some metal ions exceeding initial concentrations (i.e. $C/C_o>1$) suggesting, when at exchange capacity and working with a multi-ion solution, there is a release of less preferred ions (i.e. less competitive ions).

2.4 Filter Media

2.4.1 Selected Media

Perlite, an amorphous volcanic glass (SiO_2) formed by the hydration of obsidian, is commonly used in the construction, agriculture, food, beverage, medical, and chemical industries (Gironas et al., 2008; MEC). When heated to its softening range (760 to 1100 ^oC), perlite expands from 4 up to 20 times its original size creating a medium that is light with a high total surface area. Expanded perlite has been tested and used as a filter medium for stormwater

filtration in private and public sectors because it is cost effective and has repeatedly been proven as an effective TSS remover (e.g. approximately 79% removal efficiency) (CONTECH®, 2001, 2015; NJCAT, 2007; Gironas et al., 2008). Moreover, variations of the medium have been studied as a heavy metals' sorbent, but the overall effectiveness varies and has been shown to be highly dependent on influent concentrations. In the literature, perlite is often viewed more as a filtration medium than as an adsorptive medium.

Earthlite™ Stormwater Filter Media is a proprietary composite porous medium composed of an organic biochar and other porous materials (Sunmark Environmental). Biochar is a product produced as biomass (e.g. plant material) undergoes pyrolysis in the absence of oxygen becoming a fine grained, porous, charcoal-like material (Chen et al., 2011, Kolodynska el al., 2012). Much research has been conducted on the quality and effectiveness of biochars as a soil amendment (e.g. Beck et al., 2011). Researchers have shown the effectiveness and overall properties of biochars largely depend on not only the quality and structure of the parent materials but also on the biomass processing conditions (e.g. temperature, hold times, moisture content, organic carbon and hard carbon content). Few researchers have characterized the efficiency of the composite Earthlite™ filter medium, but research conducted by Gray et al. (2015) on biochars used by Earthlite™'s manufacturer has shown that at typical, natural infiltration rates it can remove approximately 90% copper and 51% zinc (dissolved). Other researchers have suggested that high biochar sorption

capacities of heavy metals are due to the large amount of oxygen containing groups on the surface of biochar (Liu and Zhang, 2009; Kolodynska el al., 2012).

Filter33™ is a proprietary granular adsorptive medium that proposes removal efficiencies of 88%, 96%, and 87% for copper, zinc, and TSS, respectively (Clarus Water Solutions, 2015). Additionally, it is reported to be able to handle acidic waste and a wide range of flow rates (2 to 200 gpm). Currently, it is being used in industrial environments.

2.5 Removal Mechanisms: Previous Studies

2.5.1 Perlite

The complete chemical composition of perlite as outlined by Alkan and Dogan (2001) is shown in Table 1 with the primary constituents being SiO_2 (71-75%) and Al_2O_3 (12.5-18%).

Table 1. Chemical composition of perlite (Alkan and Dogan, 2001).

Constituent	Percentage present
SiO_2	71–75
Al_2O_3	12.5–18
Na_2O	2.9–4.0
K_2O	4.0–5.0
CaO	0.5–2.0
Fe_2O_3	0.1–1.5
MgO	0.03–0.5
TiO_2	0.03–0.2
MnO_2	0.0–0.1
SO_3	0.0–0.1
FeO	0.0–0.1
Ba	0.0–0.1
PbO	0.0–0.5
Cr	0.0–0.1

The silicon atoms attach to monovalent hydroxyl groups creating the silicon groups: hydroxyl, silanediol and silanetriol as shown below.

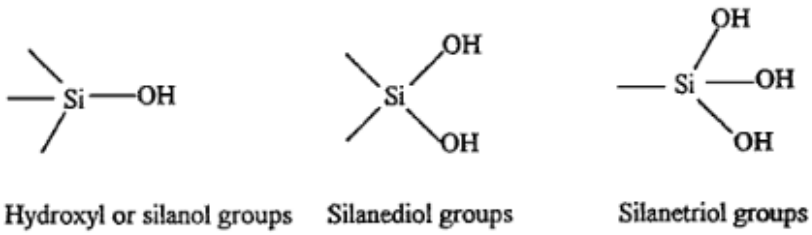

Figure 2. Silicon groups at the surface of perlite (Alkan and Dogan, 2001).

The alumina atom is proposed to have the following hydrous oxide surface groups:

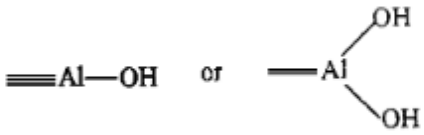

Figure 3. Alumina hydrous oxide surface groups (Alkan and Dogan, 2001).

These surface hydroxyl groups are primarily responsible for the sorption of metal ions in perlite. Furthermore, since these are surface events and hydroxyl groups are easily accessible, perlite sorption tends to be rapid.

Previous copper perlite studies have reported an optimal pH of 5 for maximum removal (e.g. sorption capacity) and noted that copper hydroxide precipitates occur above this pH (Sari et al. 2007; Swayampakula et al., 2009). In kinetic batch tests, removal efficiencies for multiple metals including copper were

seen to plateau between 90 and 150 minutes which lead researchers to suggest that the sorption follows pseudo second order (PSO) kinetics (Mathialagan and Viraraghavan, 2002; Sari et al. 2007; Ghassabzadeh et al., 2010). A study of chitosan-coated perlite beads using binary and tertiary solutions observed more favorable adsorption for Cu(II) as compared to Co(II) and Ni(II) in both kinetic batch and column studies. Moreover, the presence of another metal ion in solution decreased the adsorption capacity of the primary ion (i.e. Cu(II)), but this effect was most pronounced with Ni(II) (Swayampakula et al., 2009).

Zinc has not received as much attention in the literature due to its less aggressive nature as an ion in aquatic/aqueous systems, but one study outlines the optimal adsorption parameters found with batch tests. Zinc experienced max sorption between pH 5 and 6, which is slightly higher than that of copper. Researchers reported rapid adsorption during the first three hours followed by a plateau suggesting a rate-limited diffusion process of zinc from external to internal binding sites (Silber et al., 2012). Competitive effects of other metal ions were not tested though Zn(II) adsorption appeared to enhance phosphorous adsorption.

The long-term fate of both copper and zinc metal ions have been shown to be affected by solution pH, reaction kinetics (e.g. contact time) and/or competitive effects, suggesting that there could be a combination of specific and non-specific adsorption mechanisms contributing to their overall sorption and transport behavior.

2.5.2 Biochar

The composition and surface area of biochars differ greatly depending on the parent material used, but in general, they are composed of C, H, O, N and sometimes Si (Liu and Zhang 2009; Chen et al. 2011; Gray et al. 2015). The surface functional groups of biochar are mainly oxygen containing groups such as carboxylic, lactone and phenolic hydroxylic groups (Liu and Zhang 2009). Similar to perlite, these oxygens are responsible for metal sorption. Multiple studies suggest that the sorption follows PSO kinetics for all metals, assuming chemisorption, and that intraparticle diffusion could be the rate limiting sorption mechanism (Liu and Zhang 2009; Chen et al., 2011; Kolodynska el al., 2012).

More specifically, both Cu(II) and Zn(II) have been shown to exhibit maximum sorption capacities to biochars at a solution pH of 5 (Chen et al. 2011; Kolodynska el al. 2012). Research conducted by Kolodynska et al. (2012) on the uptake of Cu(II), Cd(II), Pb(II), and Zn(II) ions in solution to a biochar produced from pig and cow manure showed that when solution pH was below 7, there was a measured temporal variability in solution pH with pH initially increasing followed by a decrease. Researchers suggested these findings indicate ion exchange or precipitation mechanisms as part of the sorption process to the biochar. Equilibrium times for both metal ions were between 30 and 60 minutes and followed PSO as commonly reported by other researchers and mentioned previously. Additionally, in batch studies conducted by this group of researchers, as the sorbent dose was increased, the sorption capacity decreased, while the

overall sorption increased, an observation noted by others as well (Chen et al. 2011; Kolodynska el al. 2012). This is thought to be due to a conglomeration of the sorbent, decreasing individual particle surface area thereby reducing access to available sorption sites on the biochar. Interestingly, the authors suggest the subsequent measured increase in overall sorption is due to the increase in sorbent dose.

In a single copper metal solution, measured removal efficiencies approached 57-98% depending on the parent material of the biochars (Chen et al. 2011; Kolodynska el al. 2012). At low concentrations (~6 mg/L) of both metals (binary solutions), the effects of sorption capacities of one metal on the other were minimal. In binary solutions at higher concentrations, Zn(II) barely affected Cu(II) sorption capacity (Chen et al., 2011) and another study saw Cu(II) sorption changes of less than 20% in the presence of Zn(II) (Kolodynska et al., 2012). On the other hand, Zn(II) sorption was greatly impacted (decrease of 75-85%) at concentrations greater than or equal to 63 mg/L and 65 mg/L for copper and zinc, respectively (Chen et al., 2011). In all, it appears that metal ions, especially Cu(II), compete for binding sites making their sorption capacities highly solution dependent.

Biochar metals sorption, as with perlite, appear to be impacted by pH, contact time, and/or competitive effects suggesting that there could be a combination of specific and non-specific adsorption mechanisms contributing to their overall sorption capacities.

2.6 RESEARCH OBJECTIVE

Most of the published research conducted on the efficiency of filter media for removing heavy metals from solution has focused on optimizing sorption (removal) by pH manipulation. Furthermore, many of the studies have been conducted with single metal ion solutions or, when conducted using binary and tertiary solutions, the metal ion ratios in solution were at concentrations not representative of the natural environment. Additionally, many researchers have only characterized filter efficiency under static (batch) or dynamic (column) conditions while few have compared the results of these different approaches. Furthermore, much of the research conducted under flow through conditions has been performed at low flow rates thereby more closely resembling infiltration rates in the natural environment.

This research aims to characterize the potential of a mobile media filter operation for the treatment and recycling of stormwater with three primary focal points: first is to investigate removal efficiencies of various alternative filter media under induced, uniform flow conditions consistent with the performance expected for an onsite pump and treat operations. Secondly, this research characterizes the sorption mechanisms responsible for uptake in select filter media using multiple techniques such as static and kinetic batch studies plus flow through columns including flow interrupts on the measured breakthrough curves. Finally, this research represents natural stormwater conditions as much as possible in

order to represent removals that are indicative of working filter conditions. To best represent natural stormwater characteristics, solutions were modeled after pH and metal ion ratios that were found in local field samples. Likewise, a synthetic rainwater based on a local rainwater composition measurement was used as the base solution for all experimentation.

3.0 MATERIALS AND METHODS

3.1 Reagents

Copper chloride dihydrate ($CuCl_2 \cdot 2H_2O$ > 99%) and anhydrous zinc chloride ($ZnCl_2$ >95 %) were purchased from Aldrich (Milwaukee, WI) and Mallinckrodt (St. Louis, MO), respectively. Salts of ammonium sulfate ($(NH_4)_2SO_4$), sodium nitrate ($NaNO_3$), and calcium chloride dihydrate ($CaCl_2 \cdot 2H_2O$) were purchased from Fisher Scientific (Fair Lawn, NJ). Sodium sulfate (Na_2SO_4) and potassium chloride (KCl) were sourced from Sigma-Aldrich (St. Louis, MO) and Mallinckrodt (Phillipsburg, NJ), respectively. Pentafluorobenzoic acid (C6F5CO2H, 99%) was purchased from Alfa Aesar (Ward Hill, MA). Trace metal grade hydrochloric acid (HCl 36.5-38%), trace metal grade nitric acid (HNO_3 67-70%) and reagent grade sodium hydroxide (NaOH 50%) were purchased from VWR (Radnor, PA), Fisher Scientific (Fair Lawn, NJ) and EM Science (Cherry Hill, NJ), respectively.

3.2 Filter Media

Perlite, an amorphous volcanic glass formed by the hydration of obsidian, was sourced from Contech® Engineered Solutions (Portland, OR). Particle size analysis of a representative (grab) sample of Perlite characterized in this work yielded a uniformity coefficient (d_{60}/d_{10}) of 2.8. Other medium characteristics were calculated from rapid small-scale column tests (RSSCTs) yielding a bulk density of 0.18 g/cm^3, an average particle density of 0.43 g/cm^3, and a porosity of

approximately 57%. To ensure uniform and homogeneous perlite grab samples, Perlite passing an ASTM E-11 sieve no.10 (2 mm aperture) and retained on a sieve no. 40 (0.42 mm) was used in the RSSCT.

Earthlite™ Stormwater Filter Media, a commercial heterogeneous biochar medium, was sourced from Sunmark Environmental (Portland, OR). Particle size analysis of a representative (grab) sample of the medium yielded a uniformity coefficient of 5.0. Other medium characteristics were calculated from RSSCT, with an average bulk density of 0.50 g/cm^3, particle density of 1.0 g/cm^3, and an approximate porosity equal to 52%. Medium passing an ASTM- E-11 sieve no.10 (4.75 mm aperture) was used in kinetic batch tests and in the RSSCT.

Filter33™, a uniform and highly homogeneous, commercially-available granular filter medium, was sourced from Clarus Water Solutions (Portland, OR). Particle size analysis of a representative (grab) sample of the medium resulted in a uniformity coefficient of 1.9. Other medium characteristics were calculated from the RSSCT: a bulk density of 0.71 g/cm^3, an average particle density of 2.35 g/cm^3, and a porosity of approximately 70%.

3.3 Sample Collection

Stormwater samples were collected from three different catch basins on the TriMet Merlo property in Beaverton, OR (see Figure 1) at the following locations: the employee/visitor parking lot (A); the bus throughway from the washing station to the property exit (B); and immediately after the bus washing

station (C). It may be of interest to note that this final sampling location, station C, contained a CONTECH® Stormfilter. The Storm Regen® representative on site estimated that the basins had not been cleaned for approximately six months. Approximately 2 gallons of stormwater was sampled from the top half of the basin, thereby avoiding sampling from the sludge zone in the basin. Upon arrival to the lab, five discreet samples (approximately 250 mL) were taken from each stormwater container and preserved with HNO_3 to pH<2 for total metals analysis; the remaining stormwater was kept at approximately 4 ^oC (for a maximum of 7 days) for solids analysis following protocols outlined in the USEPA Industrial Stormwater Monitoring and Sampling Guide (USEPA, 2009).

Figure 4. Stormwater sample collection locations on the TriMet Merlo property in Beaverton, OR: the employee/visitor parking lot (A); the bus throughway from the washing station to the property exit (B); and immediately after the bus washing station (C).

3.4 Apparati: Filtration Studies

All filtration experiments were conducted as RSSCT in vertically-positioned acrylic soil columns (Soil Measurement Systems, Tucson, AZ), 6 cm in length with 2.5 cm inner diameter. To ensure uniform flow distribution, a fine nylon mesh followed by a porous plastic frit with distribution holes was used at the end caps for column tests done using Filter33™. Distribution plates, emplaced at the inlet and outlet of the column, for column tests conducted using Earthlite™, consisted of a fine nylon mesh followed by a layer of filter medium, approximately 8-mm thick, composed of Earthlite™ particles passing a sieve no. 4 and retained on sieve no. 10 (i.e. less than 4.75 mm and greater than 2 mm). A similar set of distribution plates, using Perlite particles retained on sieve no. 10, were created for column tests using Perlite.

Between the distribution plates, the main portion of the Perlite column was comprised of medium passing sieve no. 10 and retained on sieve no. 40. To create a homogenous core, Perlite was added in 3-4 mm layers with layer interconnection being created by touch mixer (Fisher Scientific, Fair Lawn, NJ) vibration on three equidistant outer column locations. A similar packing technique was employed for the Earthlite™ columns with medium passing a sieve no. 4 though, for layer interconnection, the column was tapped on the counter three times, rotated a third, tapped three more times; this was continued for one full rotation. The unsieved medium used in the Filter33™ columns was applied mimicking the Earthlite™ packing/interconnection technique.

3.5 Synthetic Solutions

All solutions were created using water generated from distilled water purification in a NANOpure Diamond system (Barnstead, Dubuque, IA) that creates purified water with 18.2 MΩ-cm and <5-10 ppb TOC. Prior to experimental use, the nanopure water was aerated for 8-12 hours on a Vibrax VXR orbital shaker (IKA, Wilmington, NC) or an Orbit shaker bath (Lab line, Melrose Park, IL). A recipe for a synthetic rainwater stock solution based on average ion concentration profiles of rainwater collected in the Pacific NW (Junge 1958; Junge and Werby 1958) was created using ammonium sulfate ($(NH_4)_2SO_4$), sodium sulfate (Na_2SO_4), potassium chloride (KCl), sodium nitrate ($NaNO_3$), and calcium chloride dihydrate ($CaCl_2 \cdot 2H_2O$) (Table 1).

Table 2. Ion concentrations in the synthetic rainwater and Pacific NW rainwater.

Ion	Synthetic Rainwater Concentration (mg/L)	Average Pacific NW Concentration (mg/L)
$NH4^+$	0.06	0.06
Ca^{2+}	0.19	0.19
K^+	0.06	0.06
Na^+	0.25	0.48
Cl^-	0.39	0.41
$NO3^-$	0.06	0.10
$SO4^{2-}$	0.64	0.67

Based on the reported solubility products for salts in the synthetic rainwater, several of the target concentrations were adjusted from the original recipe to ensure all ions remained in solution (i.e. minimizing precipitate formation). This stock ion solution was then diluted 1:1000 stock

rainwater:nanopure water by mass using an Ohaus Ranger 7000 (Parsippany, NJ). This synthetic rainwater was used as the background solution for all experiments and standards.

Binary solutions composed of target heavy metals, copper and zinc, were created based on the relative ratios of those metals measured in stormwater samples collected at station A (i.e. an approximate 1:4 Cu:Zn ratio). Additionally, the pH of all experiments conducted using these binary solutions was maintained at the average pH measured at the field site (pH = 6.2) (see Table 2). It may be of interest to note that the total metals concentrations of the collected stormwater at the TriMet Merlo station A were comparable to Oregon highway stormwater runoff averages reported by Nason et al. (2012).

For RSSCT experimentation, the binary metals solution (~2 mg-Cu/L and 8 mg-Zn/L) was made using metal salts ($CuCl_2 \cdot 2H_2O$ and $ZnCl_2$) dissolved in the synthetic rainwater, added by mass using an Adventurer AX 324 and/or Ohaus Ranger 7000 (Ohaus, Parsippany, NJ). A similar procedure was used to create batch binary metals solutions with initial aqueous concentrations at a wider range of concentrations and at 1:2 and 1:4 Cu:Zn metals ratios. Solution pH was adjusted using 0.1 M NaOH or HNO_3 to reach the experimentation pH of 6.2.

Table 3. Total metals of the TriMet Merlo location A stormwater and Oregon highway stormwater runoff averages reported by Nason et al. (2012).

	Merlo Station A, μg/L	Oregon Highway Runoff, μg/L
Cadmium	0.2	0.7
Copper	19	21
Lead	16	13
Zinc	85	108

3.6 Batch Experiments

Kinetic batch studies aimed to characterize the reaction chemistry (e.g. temporal variability and competitive effects) of heavy metals to Earthlite™ were conducted using a binary solution of Cu(II) and Zn(II) at a range of concentrations (19-32 mg-Cu/L and 54-119 mg-Zn/L) at binary ratios equal to approximately 1:2 and 1:4 Cu:Zn and at pH of approximately 6.2. Nalgene bottles and caps (HDPE, 250 mL) were weighed using a PJ3600 Deltarange (Mettler, Columbus, OH). Approximately 10 grams of filter medium and 100 grams of binary solution were added creating a 1:10 solids:solution ratio. The bottle was capped, gently tumbled by hand (inverted 5 times) and placed on its side in an Orbit shaker table (Lab-line, Melrose Park, IL) at 75 rpm. Reactor times started and stopped upon placement into and removal from the shaker table. The reactor's content (solids and solution) was poured through a Whatman 40 filter (8 μm retention) nested in a glass funnel. Samples were allowed to filter for approximately 10 minutes; any solution not filtered during that interval was not considered part of the sample. After filtration, a pH reading was taken followed by AAS analysis.

The batches utilized two controls, a lab blank and a medium blank, that underwent the complete batch process. The lab blank contained synthetic rainwater and the medium blank contained pH-adjusted (pH 6.2) synthetic rainwater and the medium. The measured medium blank average was subtracted from the final measured sample concentrations, respectively.

3.7 Filtration Experiments

Columns packed with either Perlite, Earthlite™ or Filter33™ media were saturated using the synthetic rainwater at 0.25 mL/min for 12-24 hours followed by 0.35 mL/min for 12-24 hours and finished at 0.5 mL/min for at least 24 hours using a Series II HPLC pump (Scientific Systems Inc., State College, PA). Uniform fluid flow through the packed columns was from bottom to top in all experimentation.

For column/flow-through experiments at flows greater than 0.5 mL/min, saturation was continued at 1.0 mL/min for a minimum of 12 hours. For studies at flows greater than 1mL/min, flow was increased in increments to help prevent preferential pathway formation. The experimental flow was held for approximately 30 minutes prior to the start of the experiment. Column weights were recorded between flow increases as well as before and after an injection or elution.

Samples were collected with a Retriever 500 (Teledyne ISCO, Lincoln, NE) or a Spectra/Chrom CF-2 (Spectrum, New Brunswick, NJ) fraction collector. It may be of interest to note, for experiments over long collection intervals (i.e. times greater than one day) these collectors accumulated a small/negligible delay error in experimental sample times. Flow rates were measured by mass on the Adventurer AX 324 (Ohaus, Parsippany, NJ). During the experiments, sample pH (including that of the influent solution and discrete effluent solution volumes) was read within 30 minutes of collection; the injection reservoir was

sampled at time increments of 5-10 hours with overall injection times requiring between one to three days total. Between sample collection/experimentation and analysis, all samples were covered and stored at 4°C.

Column experiments conducted to characterize overall fluid flow through the various select filter media were performed using a nonreactive tracer (NRT). The select packed columns were injected with a 500 mg/L PFBA solution until complete breakthrough ($C/C_o = 1$) was achieved. The columns were then eluted with PFBA-free synthetic rainwater until measured PFBA concentrations reached below our reporting limit (~1 mg/L). Duplicate NRTs were performed on Perlite column 1 (P1) and Perlite column 2 (P2) at flowrates of approximately 0.5 and 1 ml/min (P1) and at 1 and 10 ml/min (P2). Interestingly, NRT experiments using PFBA were attempted on the Earthlite™ and Filter33™ columns; both media reacted with the available tracer (PFBA).

Perlite columns 1, 2 and 3 (P1, P2 and P3) were injected with the binary metals solution (~2 mg-Cu/L and 8 mg-Zn/L, pH~6.2) at 10, 10 and 1 mL/min, respectively, until complete breakthrough ($C/C_o = 1$) of zinc was achieved (approximately 10 pore volumes injected). Flow interrupts lasting approximately 24 hours were performed on P2 and P3 during the injection but after complete breakthrough of zinc. Perlite columns P1 and P2 were eluted with synthetic rainwater until zinc readings on the AAS were below the reporting limit (~<0.1 mg/L).

Earthlite™ columns 1, 2, 3 and 4 (E1, E2, E3 and E4) were injected with

the binary metals solution (~2 mg-Cu/L and 8 mg-Zn/L, pH~6.2) at flowrates equal to 3, 5, 1, and 3 ml/min, respectively. The binary metals solution was injected for approximately 220, 400, 460, and 430 pore volumes (i.e. bed volumes), respectively. Flow on E4 was interrupted for ~25 hours during this initial injection. A PFBA injection was performed on Earthlite™ column 5 (E5) at 5 mL/min for approximately 12 pore volumes (PV).

Filter33™ columns 1, 2 and 3 (F1, F2, and F3) were injected with approximately 400, 1900 and 1700 pore volumes of the binary metals solution (~2 mg-Cu/L and 8 mg-Zn/L, pH~6.2). These flow-through experiments were conducted at average flowrates of 1, 10, and 10 ml/min, respectively. After complete breakthrough was measured for zinc ($C/C_o = 1$) in F2, multiple flow interrupts were conducted, each lasting between 6 to 8 days in total. Discrete samples were collected following these flow interrupts, measuring rebounding/recovering concentrations in the effluent. Following each flow interrupt, F2 was flushed with the binary metals solution for an additional 360 to 900 pore volumes. After a total of approximately 4800 pore volumes of binary metals solution injection, F2 was eluted with metals-free synthetic rainwater as follows: 45 PV at 10 mL/min, 25 PV at 0.5 mL/min, 3 day flow interrupt, 5 PV at 10 mL/min. A PFBA arrival and elution at 10 mL/min immediately followed the final rainwater elution on F2.

F3 was eluted at 10 mL/min in the following manner: synthetic rainwater (50 PV), nanopure water (50 PV), 12 day flow interrupt, nanopure water (50 PV),

20 day flow interrupt, synthetic rainwater (35 PV). A PFBA arrival, 13 day flow interrupt, elution at 10 mL/min followed the final rainwater elution on C3.

3.8 Sample and Data Analysis

3.8.1 Particle Size Analysis

A particle size analysis was performed on Perlite, Earthlite™ and Filter33™ media following the American Society for Testing and Materials (ASTM) procedures C136-01 and D2487-10 using ASHTO E-11 sieves 1/4", 4, 6, 10, 40, 100, 150 and 200 (ASTM 2001, 2010).

3.8.2 Solids Analysis

Solids analysis was performed on the stormwater per section 2540 B, C and D of the Standard Methods for the Examination of Water and Wastewater (APHA, 2012). Total suspended solids (TSS) samples were processed using a 300 mL glass funnel and base (Kimble Kontes LLC, Vineland, New Jersey) with a 1.2 μm retention filter (MilliporeSigma, Burlington, MA). Total solids (TS) were weighed and dried in glass beakers. Sample weights were recorded using an AJ100 analytical balance (Mettler, Columbus, OH) after drying in an International 1350F convection oven (VWR, Radnor, PA). For QA/QC, all samples were measured in triplicate and redried/reweighed until the measured mass difference was less than 4%.

3.8.3 Sample Analysis

PFBA was analyzed using a U-1800 UV-Visible spectrophotometer (Hitatchi, Tokyo, Japan) at a wavelength of 226 nm. Standardization of the UV-Vis was achieved by calibrating the instrument to a 10-point standard curve with concentrations ranging from 1 to 525 mg/L. To stay within the instruments linear response range, samples and standards above 175 mg/L were diluted 1:3 using PFBA-free synthetic rainwater. Synthetic rainwater was analyzed every 10 samples to track and adjust for any quantifiable baseline shifts.

Stock solutions of 500.14 mg-Cu/L and 500.57 mg-Zn/L liter were made using copper and zinc salts ($CuCl_2 \cdot 2H_2O$ and $ZnCl_2$), nanopure water and HNO_3 on an AJ100 analytical balance (Mettler, Columbus, OH). Standardization of the AA-7000 Atomic Absorption Spectrophotometer (Shimadzu, Kyoto, Japan) was achieved by calibrating the instrument to a 9-point copper and a 10-point zinc standard curve with concentrations ranging from approximately 0.1-8 mg Cu/L and 0.1-2 mg Zn/L. Copper and zinc samples from the batches, digests and transport studies were analyzed at wavelengths of 345.8 and 636.2 nm, respectively.

Every 10-15 samples, standard checks and metals-free synthetic rainwater blanks were read to ensure a less than 10% error and to track quantifiable baseline shifts, respectively. Baseline shifts, as absorbance measured using synthetic rainwater, were subtracted from sample absorbance, accordingly. Samples that were outside of the calibration curve range were

diluted by mass using the Adventurer AX 324 (Ohaus, Parsippany, NJ) with synthetic rainwater prior to analysis.

Sample pH readings were taken using a SympHony pH probe (VWR, Radnor, PA) in combination with a 420A pH meter (Orion, Beverly, MA) or using a HI 98190 pH/ORP meter (Hanna, Woonsocket, RI).

3.8.4 Digests

Filter media collected after binary metals solution column tests were digested according to ISO 11466.3 method as outlined by Pena-Icart et al. (2011) to quantify total metals concentrations. Sample size was increased from the protocol (0.25 to 1 g) to achieve a more representative grab sample; acid volumes were increased to reflect this change. The solids were air dried prior to digestion. Samples were digested on Central Scientific hotplate (Chicago, Illinois) and analyzed by AAS. Digest blanks and spikes were employed to account for procedural background and recovery.

3.8.5 Data Analysis

3.8.5.1 Batch Experiments

In kinetic batch experiments, the overall uptake/removal of target heavy metal in solution (reported as mass of metal removed relative to mass of sorbent) was determined by mass difference for each time step at all ratios and concentrations of copper and zinc. Based on a Visual MINTEQ analysis of metals

solution chemistry at solution pH equal to 6.2, performing a mechanistic analysis of sorption in these experiments is complicated, at minimum, by the potential for metal precipitate formation. Consequently, metal uptake herein is referred to as removal. Metals removal was determined using the commonly employed mass balance expression:

$$metals\ removal = q_t = \frac{(C_o - C_t)V}{m} \quad (3)$$

where q_t is the removal at time t (mg/g), C_o is the initial solution concentration (mg/L), C_t is the solution concentration at time t (mg/L), V is the volume of metals solution (L) and m is the mass of the solids (g). Additionally, the percent of metals removal was determined as follows:

$$\%\ metals\ removal = \left(\frac{(C_o - C_t)}{C_o} * V\right) * 100 \quad (4)$$

with all variables as previously described.

Target metal removals were modeled using a pseudo second-order (PSO) expression as described in Equation 5.

$$\frac{t}{q_t} = \frac{1}{k_2 q_e^2} + \frac{t}{q_e} \quad (5)$$

where q_t is metals removal at time t (mg/g), q_e is long-term, maximum, metals removal (mg/g), and k_2 is the second-order reaction rate coefficient (g/(mg-min)). The values of k_2 and q_e describing the temporal variability and long-term,

maximum metals removal were determined using linear regression analysis of measured mass removals expressed as t/q_t (min g/mg) verse time (min).

The retardation factor (R), often used to qualify transport behavior of reactive pollutants through porous media, was calculated using data collected from the batch experiments as follows:

$$R = 1 + \frac{\rho_b K_D{}^*}{\theta} = 1 + \frac{\rho_b \left(\frac{q_e}{C_e} * 1000\right)}{\theta} \quad (6)$$

where ρ_b is the medium's measured dry bulk density (g/cm^3), $K_D{}^*$ is defined as the apparent equilibrium distribution coefficient describing the overall distribution of mass between sorbent and solution phase, q_e is the measured equilibrium (maximum) metals removal (mg/g), C_e equals the equilibrium solution concentration of target heavy metal (mg/L), and θ is defined by the volumetric water content of the filter medium.

3.8.5.2 Filtration Experiments

Moment analysis of measured breakthrough curves for target heavy metal transport through the filter media was conducted to estimate mass removals and to qualify overall transport behavior. The zeroth moment of measured, complete breakthrough curves describes the total mass recovered and was calculated as follows:

$$M_0 = \int C^* dT = \sum \overline{C^*} \, \Delta T \quad (7)$$

The first moment, providing information on the center of mass and its arrival time, was calculated using:

$$M_1 = \int C^* T dT = \sum \overline{C^* T}\, \Delta T \quad (8)$$

The normalized first moment, representing the apparent residence time of the system, was calculated as:

$$\frac{M_1}{M_o} = \frac{\int C^* T dT}{\int C^* dT} = \sum \frac{\overline{C^* T} \Delta T}{C^* \Delta T} \quad (9)$$

In the above moment analysis, C^* is nondimensional concentration (C/C_o) and T is nondimensional time expressed as pore volumes (PV).

The retardation factor was determined for those transport experiments resulting in complete breakthrough curves (defined for those measured breakthrough curves exhibiting complete mass recovery) using the corrected first moment. For example, the retardation factor describing the transport of PFBA through Perlite was calculated using Equation 10.

$$R = \frac{M_1}{M_o} - \frac{1}{2} PW \quad (10)$$

where M_1 and M_0 are as defined previously and PW is defined as the nondimensional pulse width (i.e. the pore volumes of solution injected/input into the column). Additionally, given complete breakthrough (with measured concentrations in the effluent approaching $C/C_o = 1$), estimates of the retardation

factor was determined by calculating the area above the measured arrival wave using the following zero moment:

$$M_o = \int (1 - C^*) dT = \sum \overline{(1 - C^*)}\, \Delta T \quad (11)$$

with all parameters as described previously.

Finally, an estimate of the long-term, maximum, metals removal (q_e), as defined previously, achieved following complete breakthrough ($C/C_o = 1$) of target metals through the filter media) was determined as the area above the measured breakthrough curve for target metals relative to the column medium mass (see Equation 12).

$$\frac{M_o}{m} = \frac{\int (1-C) dV}{m} = \frac{\sum \overline{1-C}\, \Delta V}{m} \quad (12)$$

where C is the measured concentration of the target heavy metal (mg/L) and V is the volume of solution pumped through the filter medium (L) and m is the total mass of medium in the column (g).

3.8.5.3 Digests

The digests were used to estimate the metal removal and the percent metals removal of the media in the Perlite and Earthlite™ RSSCT. In both calculations, it was assumed there was uniform metals distribution in each layer. The metals removal was calculated:

$$metals\ removed = \frac{\sum\left(\frac{m_{metal}}{m_{solids}} * m_{layer}\right)}{m} \quad (13)$$

where m_{metals} is the mass of metals in the digest sample (mg), m_{solids} is the mass of solids in the digested sample (g), m_{layer} is the mass of solids in the layer (g) and m is the total mass of solids in the column (g).

The percent metals removed was estimated from the following relationship:

$$\%\ metals\ removed = \left(\frac{\frac{m_{metal}}{m_{solids}} * m_{layer}}{PW * C_o}\right) * 100 \quad (14)$$

where m_{metals} is the mass of metals in the digested sample (mg), m_{solids} is the mass of solids in the digested sample (g), m_{layer} is the mass of solids in the layer (g), PW is the pulse width (L) and C_o is the initial concentration (mg/L).

4. RESULTS AND DISCUSSION

4.1 Filtration Experiments

The measured effluent concentrations of target heavy metals reported in the following discussion are of total metals and as such will be referred to as copper and zinc throughout.

4.1.1 Nonreactive Tracer

Nonreactive tracer (NRT) experiments were performed to characterize the overall hydrodynamics of fluid flow in the rapid small scale column tests. These experiments also served to qualify the overall reproducibility between discrete column tests. Tracer experiments conducted in duplicate on Perlite column 1 (P1) and Perlite column 2 (P2) yield similar arrival waves with a small, reproducible degree of dispersion for each RSSCT, independent of discrete packing and flowrate (Figure 5). These findings were further supported by modeling results (e.g. moment analysis and numerical modeling to the advection dispersion equation) of the overall physical hydrodynamics (results not shown).

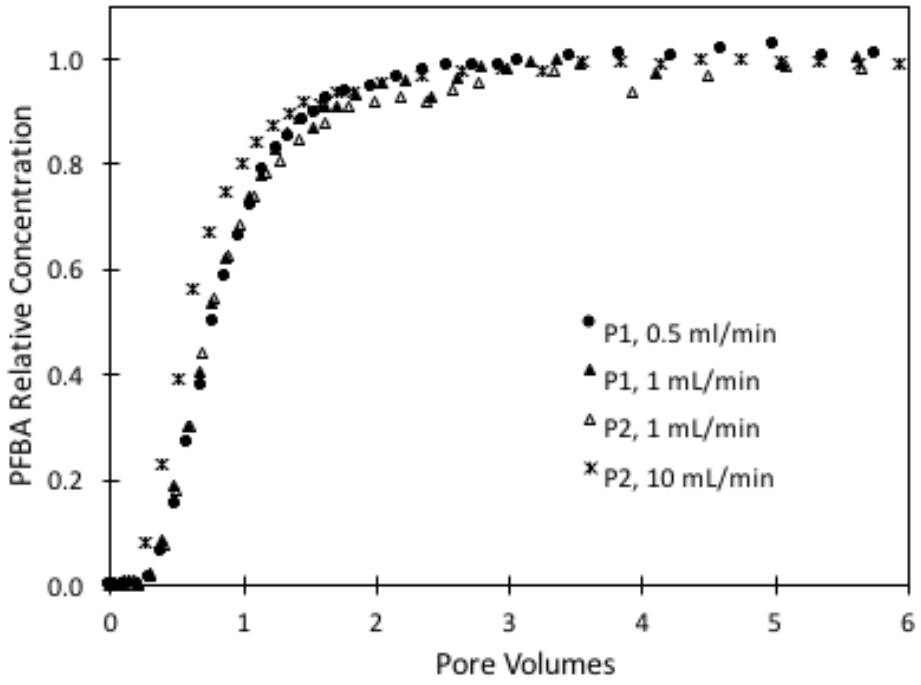

Figure 5. PFBA breakthrough curves for Perlite systems at various pore-water velocities to characterize the overall hydrodynamics of fluid flow.

4.1.2 Metals

4.1.2.1 Perlite

The breakthrough curves for the transport of zinc obtained from multiple Perlite columns are essentially identical suggesting that the transport and overall removal of zinc was reproducible and that changes in approach velocity (i.e. an order of magnitude increase in flow from 1 to 10 mL/min) do not significantly impact the zinc-Perlite interaction (see Figure 6, wherein representative nonreactive tracer results are included for comparison). Analysis of the measured breakthrough curves for zinc through Perlite, with zinc approaching C/Co=1 after

approximately five pore volumes of injection, yielded retardation factors (R values using Equation 11) approximately equal to one.

While the overall copper transport through Perlite is described by incomplete breakthrough, with a long-term, steady state concentration plateau (copper concentrations gradually approaching C/Co=0.8), copper's measured transport behavior was reproducible and not significantly impacted by approach velocity (Figure 7). A model of the binary metal injection solution using Visual MINTEQ revealed the potential for precipitation of copper oxide (CuO), indicating precipitation of copper species from solution could be responsible for the concentration plateau (i.e. the difference in C_o to C_{max}). As mentioned previously, much of the research conducted using Perlite in batch studies have been conducted at a pH of 5 due to copper complexation (Sari et al. 2007; Swayampakula et al. 2009). With the overall goals of this research being to model natural stormwater systems, the pH throughout these experiments was maintained at pH equal to 6.2.

Figure 6 shows the results of experiments conducted with the binary heavy metals solution compared to measured effluent pH. The effluent pH dropped rapidly in the first two pore volumes to a pH of 5.6 and gradually recovered to achieve the injection pH (pH=6.2) at approximately the same arrival of the metals' steady state plateaus in concentration. The measured pH drop and subsequent rise could indicate a proton (H^+ ion) release created by the Perlite-metals interaction combined with an insufficient medium buffering capacity.

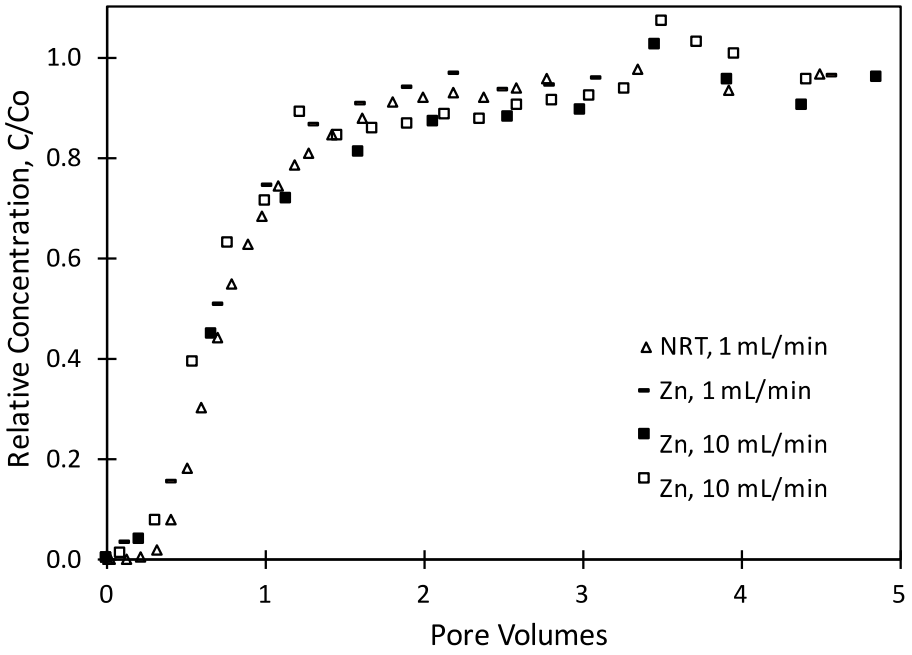

Figure 6. Breakthrough curves for zinc transport in Perlite columns. A representative NRT breakthrough curve is included for comparison.

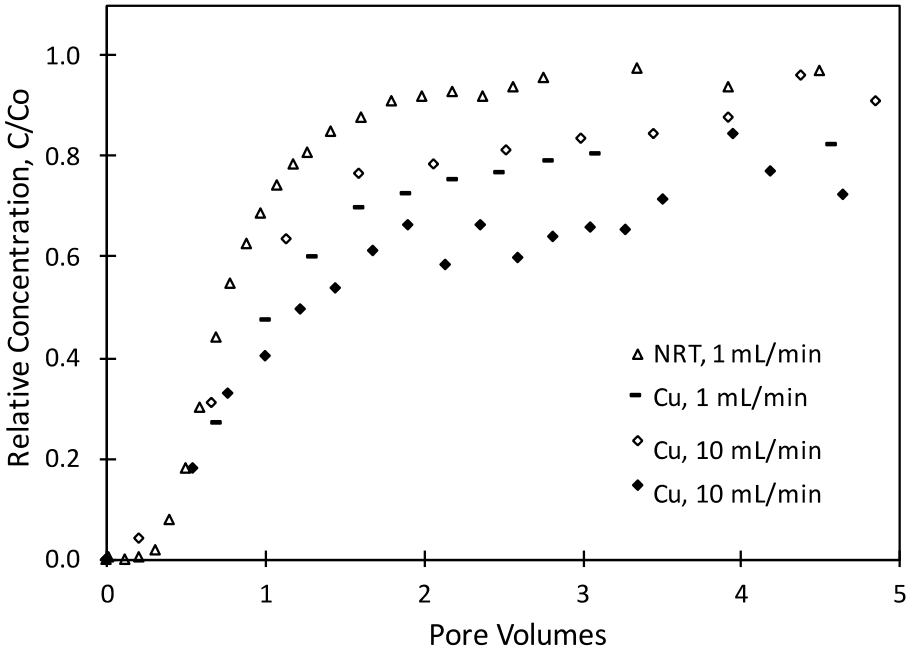

Figure 7. Breakthrough curves for copper transport in Perlite columns. A representative NRT breakthrough curve is included for comparison.

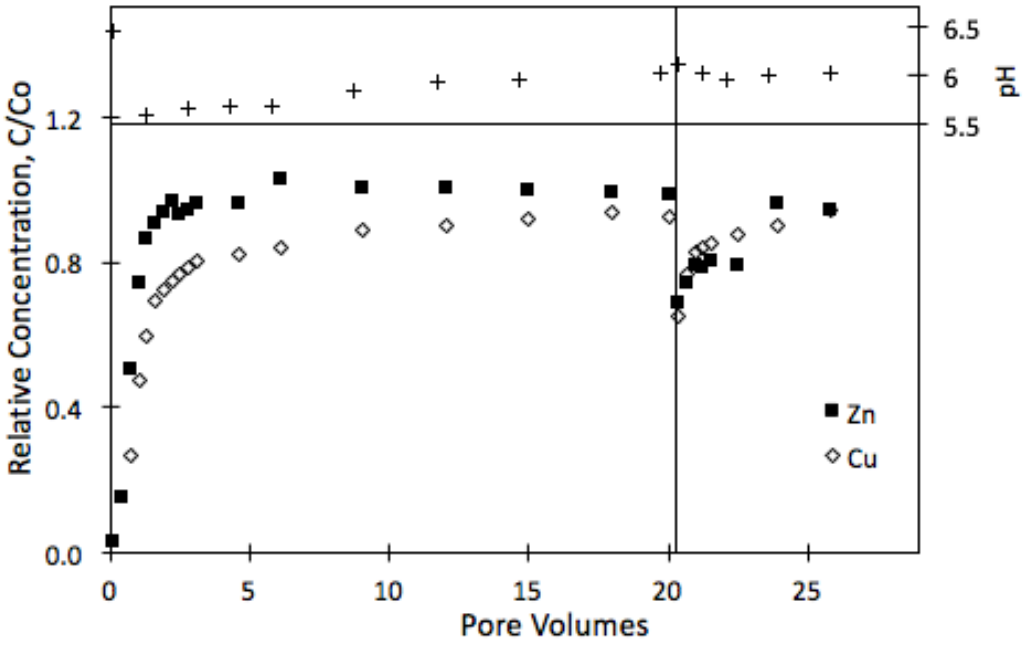

Figure 8. Measured breakthrough curves for copper and zinc with a 24-hour flow interrupt (represented by a vertical black line) at approxmently 20 pore volumes. Representative effluent pH readings are included. Experiment was conducted at an average flowrate equal to 10 mL/min.

The results of a 24-hour flow interrupt followed by continued injection of the binary metals solution conducted on P3 are shown in Figure 8. Effluent concentrations of both target metals decreased in the resident fluid followed by a rapid return to pre-interruption concentrations in less than five pore volumes. Analysis of rebounding metals concentrations assuming first order reaction kinetics produced reaction rate constants (k_1) of 0.0032/min with an $R^2 = 0.82$ and 0.0028/min with an $R^2 = 0.59$ for zinc and copper, respectively. These results suggest physical sorption and/or ion exchange reactions occur during the static state. The overall target metals' transport behavior measured through Perlite

suggests that nonspecific sorption mechanisms dominate. The observed uptake and evidence of mass loss (indicated by the measured steady-state plateau of copper at C/Co=0.8, for example) in comparison to other studies published in the literature could be due to the use of test parameters mimicking the natural environment versus testing under optimized filtration conditions as commonly reported in the literature (i.e. optimized pH, contact time, temperature and sorbent dose) (e.g. Alkan and Dogan, 2001; Ghassabzadeh et al. 2010; Sari et al. 2007).

4.1.2.2 Earthlite™

The measured arrival waves for the transport of zinc through Earthlite™ obtained from multiple rapid small-scale columns have comparable shapes yet show an approach velocity dependent removal efficiency such that as fluid flow decreases Earthlite™ exhibits greater overall removal efficiencies (see Figure 9). For example, complete removal of zinc was measured after approximately 100 bed volumes at influent flowrate equal to 1 mL/min (with breakthrough of zinc occurring thereafter), while said breakthrough occurred after approximately 30 bed volumes as the flowrate was increased to 5 mL/min. Additionally, apparent retardation factors (using Equation 11) for zinc equaling 130 and 240 for flowrates of 5 and 1 mL/min, respectively, support this trend, wherein the measured transport of zinc through Earthlite™ is impacted by the fluid flowrate.

These results suggest the presence of a rate-limited sorption mechanism for the removal of zinc.

Interestingly, measured concentrations of copper in the effluent of Earthlite™ column tests showed extremely delayed and minimal breakthrough in comparison to zinc, highlighting the competitive nature of copper in the binary heavy metal solution (Figure 10). Furthermore, effluent pH measured throughout column experiments conducted with the binary solution exhibit an initial rise in pH (pH~6.2 to pH~8.9) followed by a gradual decrease/recovery to a pH of approximately 6.9. That measured recovery in pH coincides with the zinc concentration plateau measured in the effluent (Figure 9). These results possibly indicate the exhaustion of instantaneous mechanisms (i.e. nonspecific sorption

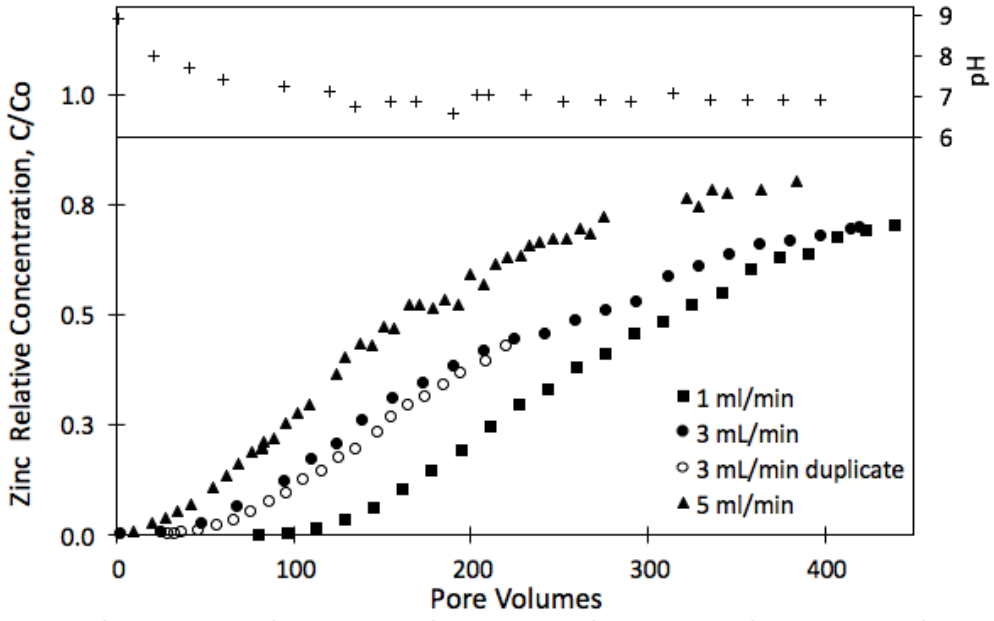

Figure 9. Zinc breakthrough curves for Earthlite™ systems at various flowrates. Representative effluent pH readings are included.

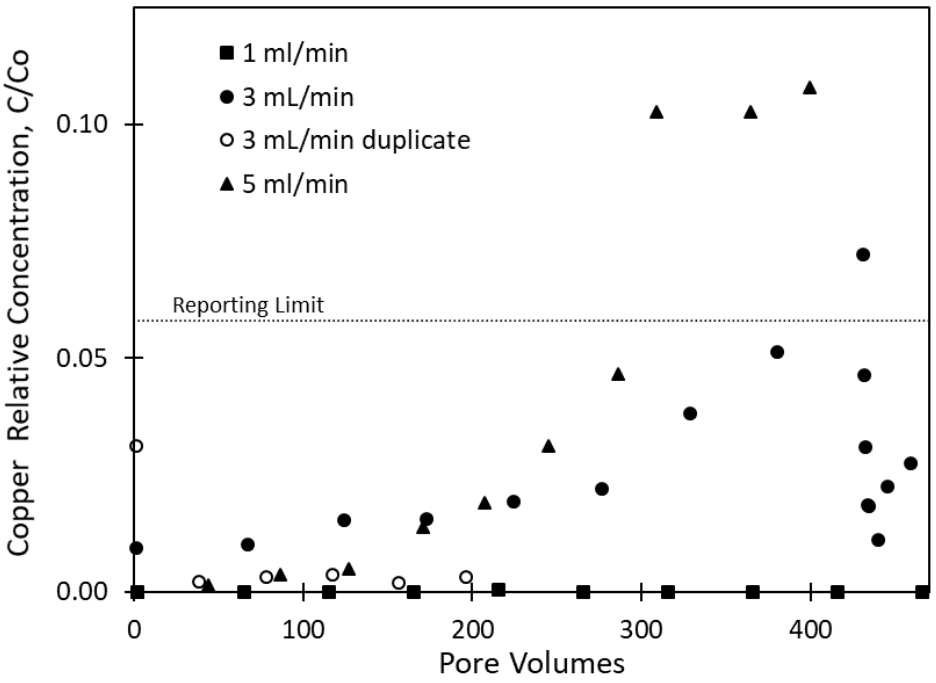

Figure 10. Copper breakthrough curves for Earthlite™ systems at flowrates including the AAS reporting limit for copper. Note the reduced ordinate axis range

.

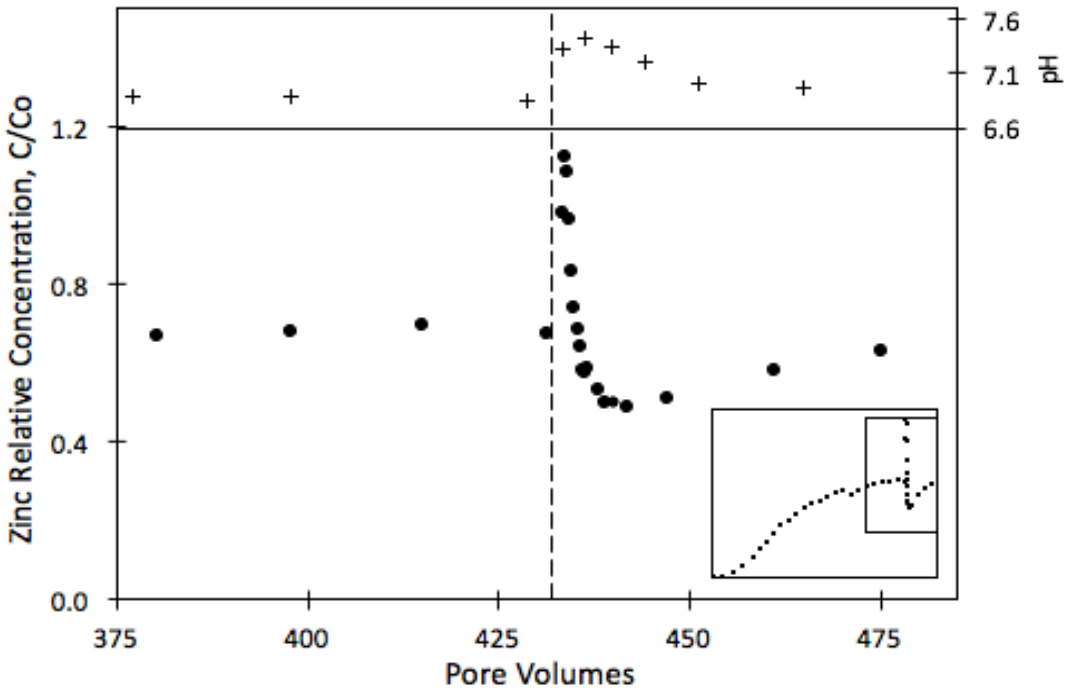

Figure 11. Effluent zinc concentrations and pH from Earthlite™ column 4 before and after a 25-hr flow interruption (represented by the vertical dashed line). An inset of the complete breakthrough curve is included for visual reference.

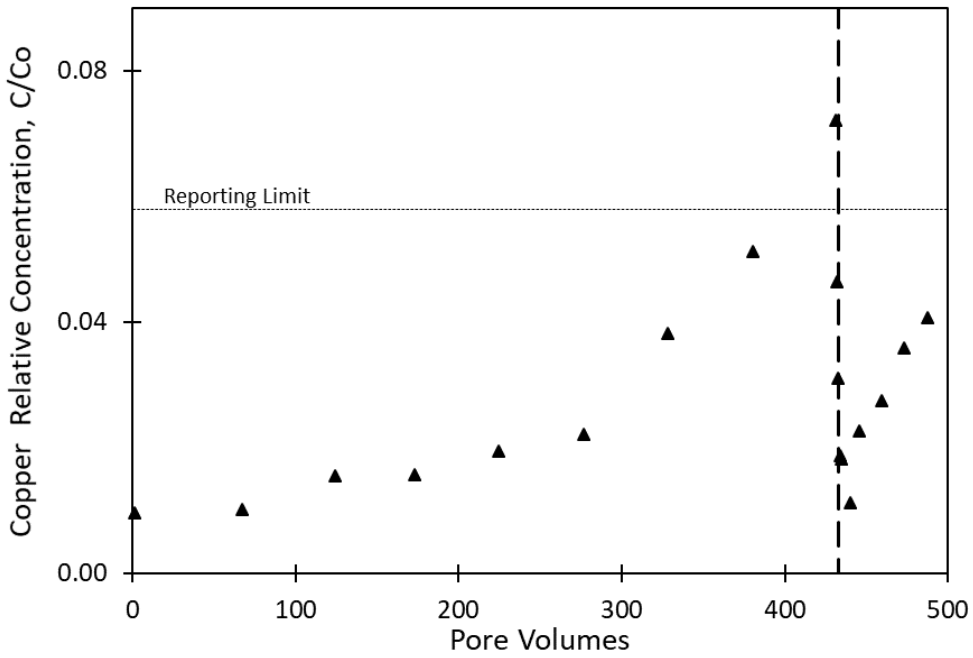

Figure 12. Effluent copper concentrations from Earthlite™ column 4 with 25-hr flow interruption (represented by the vertical dashed line) including the AAS reporting limit for copper. Note the reduced ordinate axis range.

and instantaneous ion exchange reactions) and a dominance of rate limited mechanisms.

The results of a 25-hour flow interrupt (followed by continued injection of the binary metals solution) conducted on E4 resulted in a spike (rebound) in zinc concentrations followed by a dip and gradual restabilization (recovery) to the previously measured (pre-interrupt) steady state concentration of zinc (Figure 11). Concurrently, there was a spike in the effluent pH followed by a gradual return to pre-interrupt pH. Interestingly, copper concentrations measured following this flow interrupt experienced the inverse, a dip in concentration followed by a rise in concentration immediately following the flow interruption (Figure 12). These results largely support the overall competitive effects of

copper. For example, copper overtook zinc's occupied sites on the medium resulting in a higher concentration of zinc in the resident fluid and a lower overall copper concentration. Thereafter, additional binary metal solution (e.g. more copper) was introduced creating a competitive takeover of additional zinc sites which presented as elevated zinc (and decreased copper concentration) post resident fluid flush (in comparison to pre-interrupt conditions). Moreover, the observed post interrupt pH trend suggests ion exchange equilibrium occurred in the static state (e.g. giving time for protons (H^+ ions) to participate in the interaction). Gu et al. (1995) saw similar competitive displacement and concentration spikes in column experiments as sorption sites became limited while the working solution contained multiple species with differing uptake potentials (a snow plow effect).

4.1.2.3 Filter33™

The results from the initial Filter33™ RSSCT (F1) conducted at 3 mL/min showed that after nearly 400 PV of binary metals solution injection, effluent concentrations of both target heavy metals remained below reporting limits (results not shown). Subsequently, columns F2 and F3 were conducted at an increased flowrate (10 mL/min), one closely modeling (scaled for size) the flowrates expected in the mobile treatment unit. The measured transport behavior of zinc through the Filter33™ medium (columns F2 and F3) exhibited similar overall behavior in that the initial zinc breakthrough began near 700 PV

followed by inflection at approximately 1100 PV (Figure 13). F2 exhibited a slightly greater degree of spread which translated into a slight delay in complete breakthrough (C/Co=1) Regardless, both columns had retardation factors of approximately 1100 (as described in Equation 11). Effluent pH measured throughout the column tests displayed an initial rise in pH (pH~6.2 to pH~7) followed by a gradual decrease/recovery to the injection pH coinciding with the complete breakthrough of zinc.

Multiple, long-term flow interrupts were conducted on F2. Measured concentrations of zinc (including dipping, rebounding, and recovering) showed overall reproducible transport behavior. For example, following flow interrupt 1 and 2, there was a measured drop then peak in zinc effluent concentrations ($C/C_o>1$) followed by a decrease/recovery to a slightly higher than pre-interrupt concentration plateau (Figure 15). The final two flow interrupts exhibited a similar trend but with a later peak without a subsequent decrease in measured concentrations. Concurrently, copper arrived in the effluent (i.e. broke through) after approximately 4000 bed volumes of solution indicating preferential uptake wherein zinc's initial breakthrough occurred in approximately one-sixth of the time of copper's (Figure 14). With each flow interrupt, the magnitude of the initial zinc concentration drop decreased possibly portraying an approach to the medium's zinc capacity and/or the competitive filling of sites by copper during the flow interruption. The measured peaks in zinc concentration following the long-term flow interrupts could be due to the aforementioned snow plow effect.

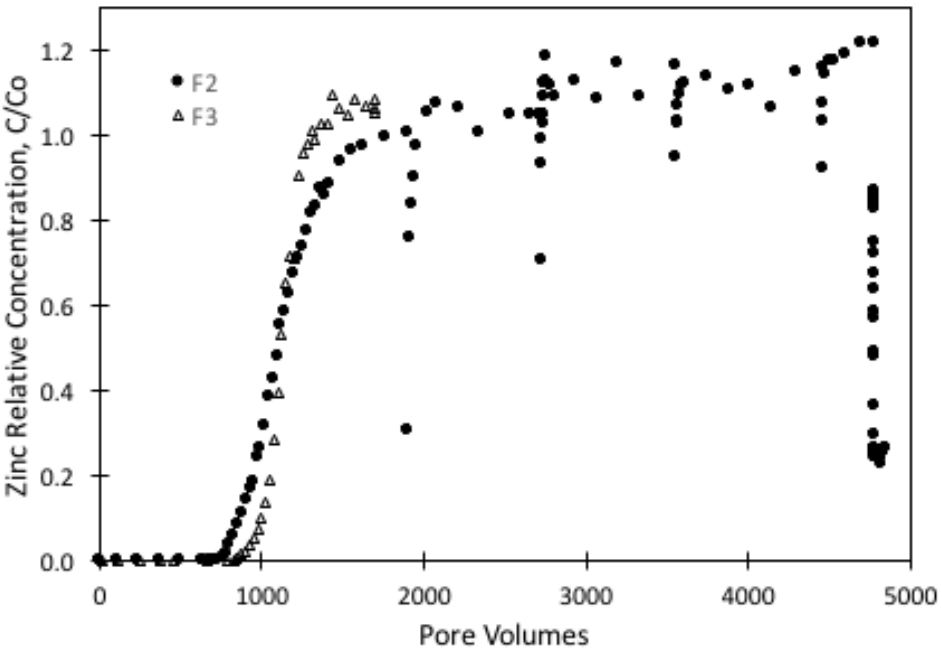

Figure 13. Complete zinc breakthrough curve for Filter33™ column 2 (F2) including four flow interruptions and initial elution. Column 3 (F3) was a duplicate of F2; both experiments were executed at 10 mL/min.

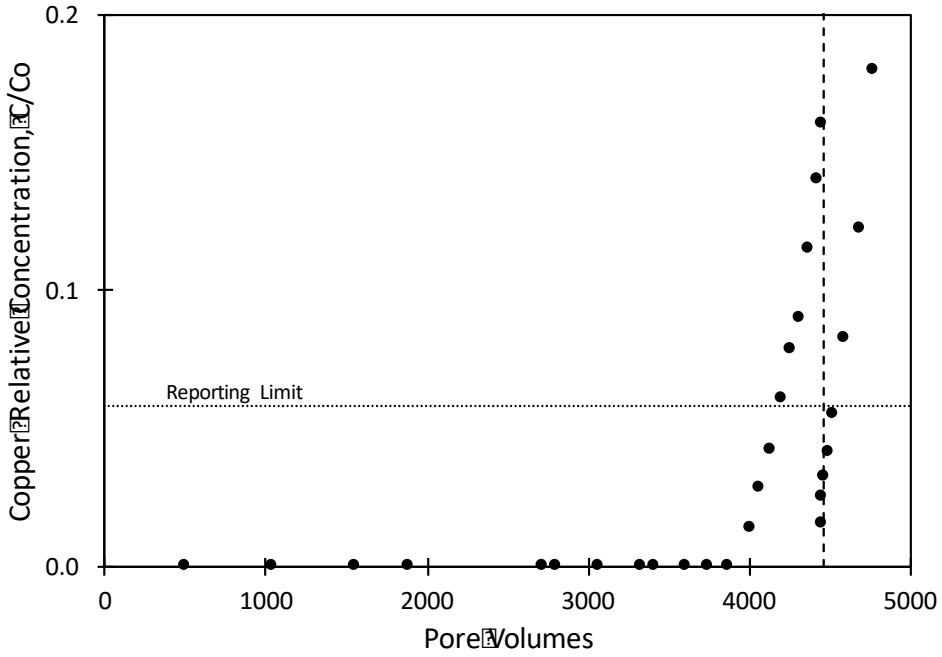

Fig. 14. Effluent copper concentrations from F2 with an 8-day flow interruption (represented by the vertical dashed line) including the AAS reporting limit for copper. Note the reduced ordinate axis range.

Interestingly, during the flow interrupts and subsequent reinjections, pH measured in the effluent remained relatively constant at an average of 6.04 ± 0.04 possibly indicating a spent/small ion exchange capacity such that the medium is no longer buffering the solution. Furthermore, as the columns were subsequently eluted with heavy metal-free synthetic rainwater solution, the effluent pH held around 6 while the influent pH dropped to approximately 5.3 suggesting elution desorption with a resulting ion exchange potential (i.e. an opening of sites for the H^+ ion).

Elution experiments conducted on F2 and F3 (results shown in Figure 16) again show similar overall transport behavior for zinc, independent of resident zinc concentrations in the filter media (with greater than 790 g of zinc loaded on F2 compared to 270 g on F3). The initial F2 elution displayed a dip, spike, dip, then elution tailing trend that was mimicked in a smaller overall magnitude in the subsequent F2 elutions; F3 elutions displayed a comparable trend at lower concentrations (Figure 16). These results suggest that magnitude of the elution trend and tailing concentration are related to the overall mass loaded, both being greater for F2. Additionally, the tailing concentrations could indicate a portion of rate limited desorption, more specifically, Caetano et al. (2009) suggested that elution tailing concentrations demonstrate the presence of an ion exchange controlled desorption process.

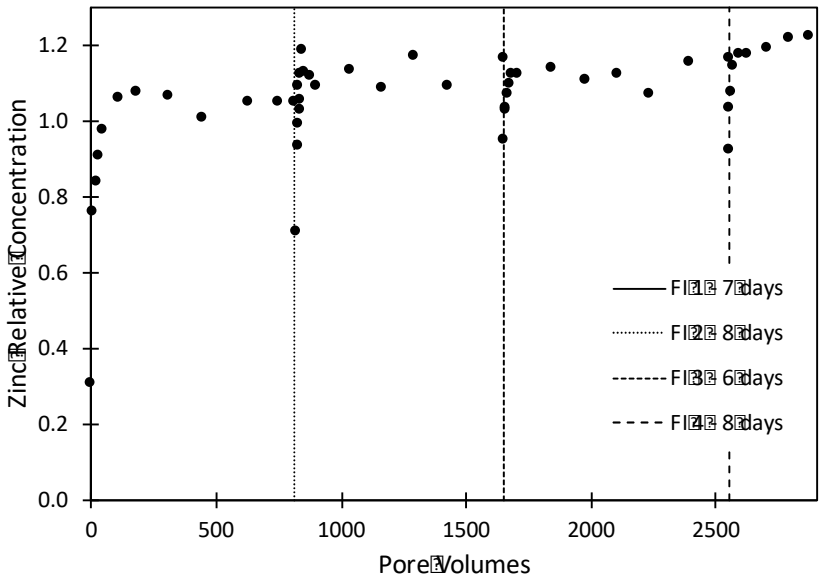

Figure 15. Effluent zinc concentrations from F2 during four discrete flow interruptions. Note that time zero on the abscissa represents the end of the first flow interruption (FI 1) and the beginning of the first reinjection.

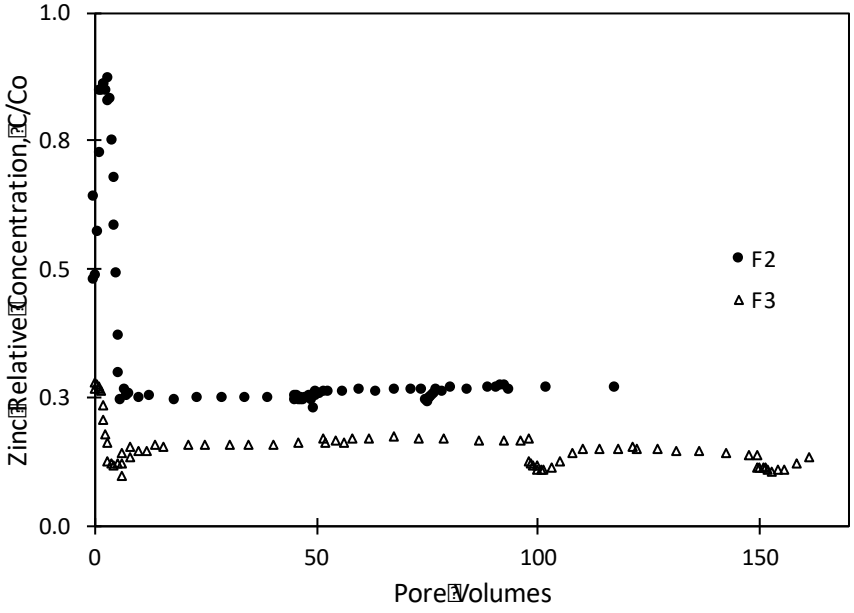

Figure 16. Zinc elutions for Filter33™ systems executed as follows. F2: 45 PV at 10 mL/min, 25 PV at 0.5 mL/min, 3-day flow interrupt, 5 PV at 10 mL/min. F3: synthetic rainwater (50 PV), nanopure water (50 PV), 12-day flow interrupt, nanopure water (50 PV), 20-day flow interrupt, synthetic rainwater (35 PV). Note that time zero on the abscissa represents the end of the binary metals solution injection and the beginning of the elutions.

4.1.3 Pentafluorobenzoic Acid

4.1.3.1 Earthlite™

A PFBA arrival on Earthlite™ column 5 (E5) showed early breakthrough and appeared to reach a concentration plateau of $C/C_o = 0.6$ after 12 pore volumes. These results indicate chemical reactions ongoing between this target organic acid species and the Earthlite™ filter medium. Batch experiments aimed to qualify the potential reaction between Earthlite™ and PFBA showed similar reaction chemistry. The arrival wave exhibited significant nonideality with a rounded front possibly indicating biodegradation mass loss possibly due to microbial content in the proprietary composite Earthlite™ filter medium.

4.1.3.2 Filter33™

Batch (static) experiments aimed to qualify the potential reaction between Filter33™ and PFBA showed negligible reaction chemistry. On the other hand, the results of column (kinetic) experiments conducted with PFBA through Filter33™ (F2 and F3 following complete characterization of target metal removal) indicate reproducible reaction chemistry and kinetics with PFBA concentrations plateauing at approximately C/Co=0.8 (i.e. without complete breakthrough) followed by an early elution concentration spike (Figure 17). Normalizing the measured effluent PFBA concentrations in F2 and F3 to their respective maximum concentrations and retardation factors, the PFBA breakthrough curves display a similar shape and inflection point again indicating

comparable transport behavior and overall removal mechanisms of this organic acid (Figure 18).

The higher C/C_o plateau measured for PFBA in F2 is thought to be related to the large amount of previously loaded mass (i.e. copper and zinc) as the medium's uptake capacity is likely spent in the core. The measured elution wave showed an early dip and spike before completely eluting, mimicking the earlier observed snow plow effect measured for the target metals (see Figure 17). Representative pH results show a pH drop coinciding with PFBA breakthrough (though it never reached the injection pH) indicting medium interaction such that it sorbed the acid and buffered the solution simultaneously (Figure 17).

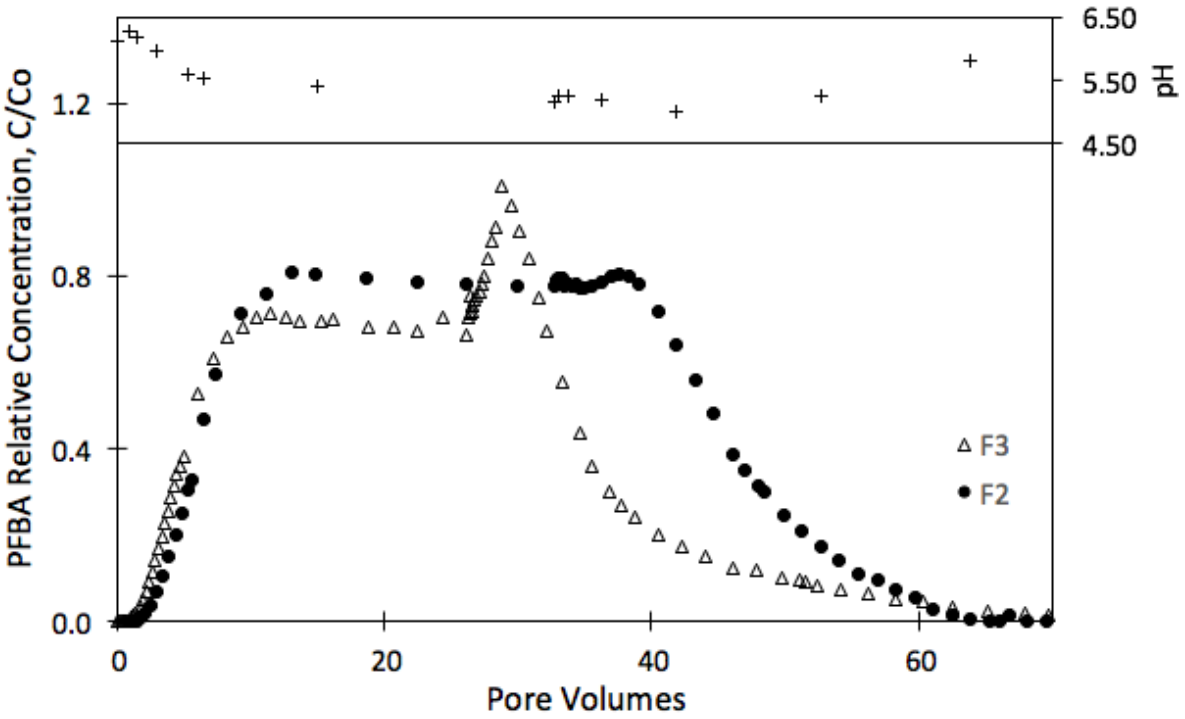

Figure 17. Complete PFBA breakthrough curves for F2 and F3 following complete characterization of target metal removal. Experimental flowrate equaled 10 mL/min. Representative effluent pH readings are included.

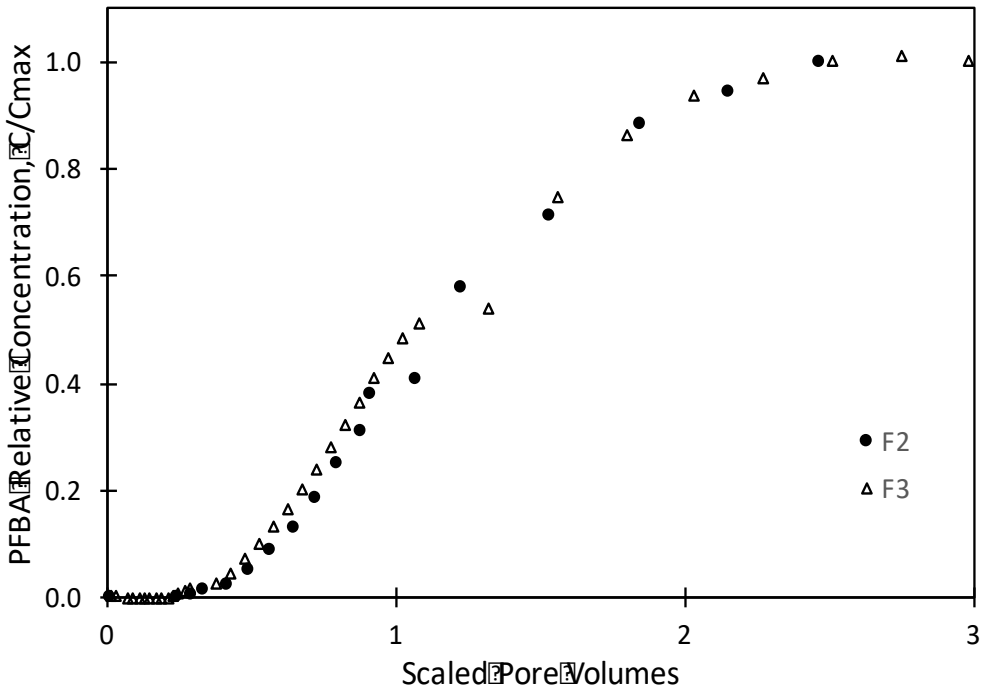

Figure 18. PFBA arrival waves for F2 and F3 normalized to their respective maximum concentrations on the ordinate and scaled by the retardation factor on the abscissa. These adjustments allow for direct comparison of transport behavior.

4.2 Filtration Experiment Comparison

4.2.1 Competitive Displacement

For all filter media tested herein, Perlite, Earthlite™ and Filter33™, there was a consistent preferential uptake of copper during the initial injection of the binary metals solution. In addition, flow interrupts conducted in Earthlite™ and in Filter33™ media resulted in a decrease in copper concentrations followed by a marked spike ($C/C_o>1$) in zinc concentrations. As previously mentioned, this drop in copper concentrations could indicate a competitive takeover of reactive sites on or in the filter medium during the static (no-flow) state followed by a continued

site dominance as new solution (e.g. more copper) was introduced to the system causing a subsequent resulting spike in zinc concentrations. Copper is small, highly reactive in its ionic form and is more stable as a complex in comparison to zinc thus an uptake preference to these composite filter media was as expected.

4.2.2 Snow plow Effects

Snow plow effects have been seen in numerous studies under different scenarios (i.e. at exchange capacity, with large changes in injection concentration, competitive displacement) suggesting that multiple factors can contribute to the phenomena. When working with metal ions, Vaaramaa et al. (2003) noted effluent concentrations exceeding initial concentrations suggesting, when at exchange capacity, there is a release of less preferred ions. Selim et al. (1992) saw a prominent snow plow effect following a large change in the concentration of the injection solution (i.e. eluting after an injection) and theorizes that this concentration change causes the matrix to release sorbed species creating a spike in effluent concentration (Starr et al. 1979). Finally, Gu et al. (1995) saw competitive displacement as sorption sites became limited while the working solution contained multiple species with differing uptake potentials.

The most prominent snow plow effects were observed after a flow interrupt was conducted in Earthlite™ and during the metals elution and PFBA elution in Filter33™ (F2 and F3, respectively) (see Figure 19). The Earthlite™

snow plow is thought to indicate a competitive site takeover by copper during the flow

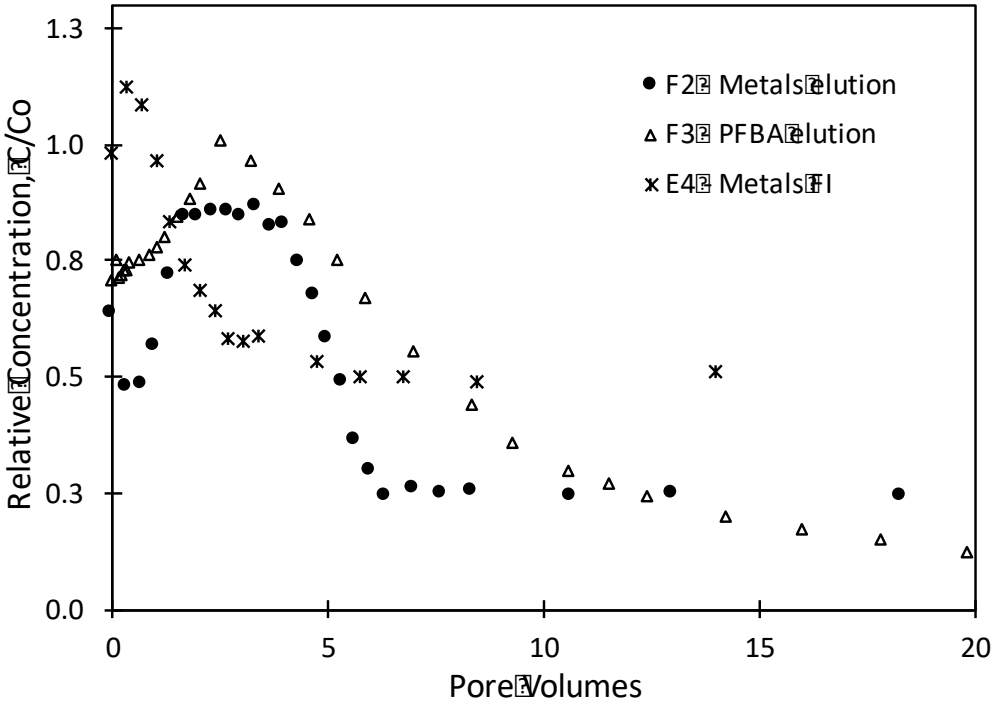

Figure 19. Observed snow plow effects in Filter33™ (F2 and F3) and Earthlite™ (E4). Note that time zero on the abscissa represents the end of a flow interruption and the beginning of a reinjection.

interruption compounded by an almost full ion capacity. The results of the snow plows measured in Filter33™ elutions suggest that the change in injection concentration and a competitive ion site takeover could have both contributed to the snow plow due to pre elution flow interrupts (each lasting approximately 29 and 13 days for F2 and F3, respectively). The results of multiple flow interrupts conducted on Filter33™ (during the F2 metals injection) showed a small degree of snow plow effects, though it was less instantaneous and significant/obvious suggesting less redistribution and competitive effects of copper as compared to

those measured with Earthlite™. Additionally, a larger part of Earthlite™'s sorption could be participating in ion exchange thus its post interrupt peak is due to both ion-exchange and sorption mechanisms, creating a peak more noticeable than those observed after the Filter33™ flow interrupts.

4.2.3 Concentration Plateau

A concentration plateau trend was observed during the Earthlite™ target metals and PFBA injections and during the Filter33™ PFBA injection possibly suggesting mass loss behavior/mechanisms in the two media. Comparing the overall transport behavior measured for PFBA in Earthlite™ compared to Filter33™ shows markedly different arrival waves (breakthrough behavior) in the two media. The nonideal shape of the arrival wave of PFBA through Earthlite™ suggests the early PFBA removal mechanisms are slightly disparate for the two media though they both display a similar long-term concentration plateau (Figure 20). Theoretically, it is possible that initially only a portion of the sites are participating in uptake and a significant portion of sorption is rate limited such that as C/C_o approaches 0.6 all of the sites are participating in uptake creating the long-term plateau. Future studies are warranted to further characterize these findings.

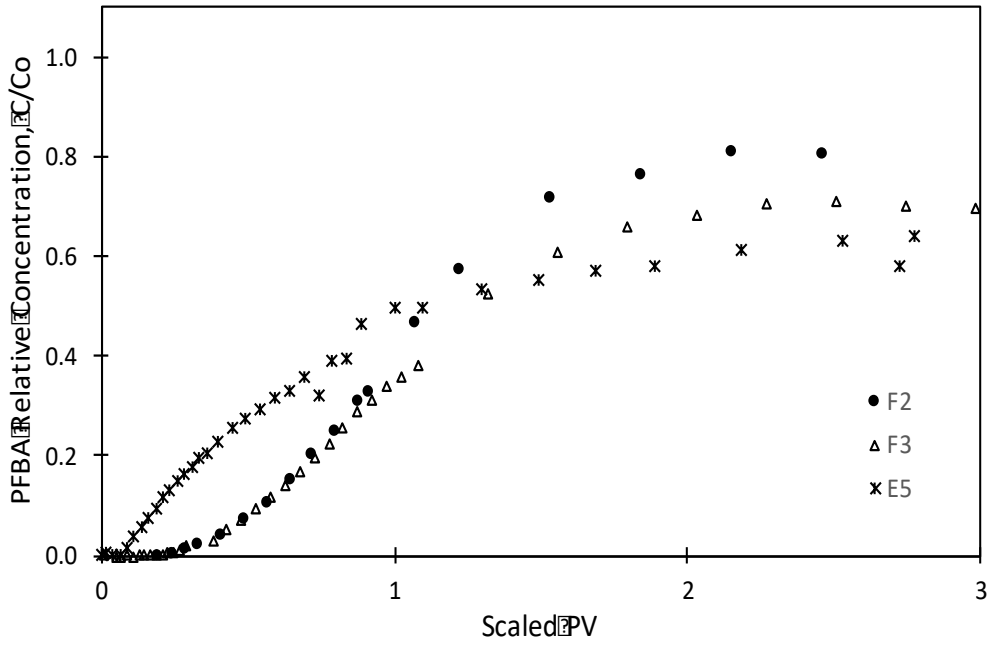

Figure 20. PFBA arrival waves for Filter33™ (F2 and F3) and Earthlite™ (E4), scaled by their retardation factors on the abscissa. These adjustments allow for direct comparison of transport behavior.

4.3 Column Digests

Digests were performed on the Perlite and Earthlite™ column media to characterize the metals distribution within each column as percent removal and removal using equations 13 and 14, respectively.

4.3.1 Perlite

The digests performed for columns P1 and P2 were grab samples from the entire core while P3 was quartered with sub samples being pulled from each quarter. P1 and P3 displayed similar zinc removal values; P2 removal was double that of the other two columns (see Table 5). The increase of removal for

P2 is thought to be related to the random nature of pulling a sub sample from the entire core and not representative of an actual increase in removal. With copper, P2 and P3 displayed similar removal values; P1 removal was higher than the other two columns (Table 5). Once again, this discrepancy is thought to be related to the sampling procedure. When looking at the percent removal for each layer, the zinc removal appears to be uniform across the column whereas the copper removal is greatest at the bottom of the column where the injection was occurring (Figure 21).

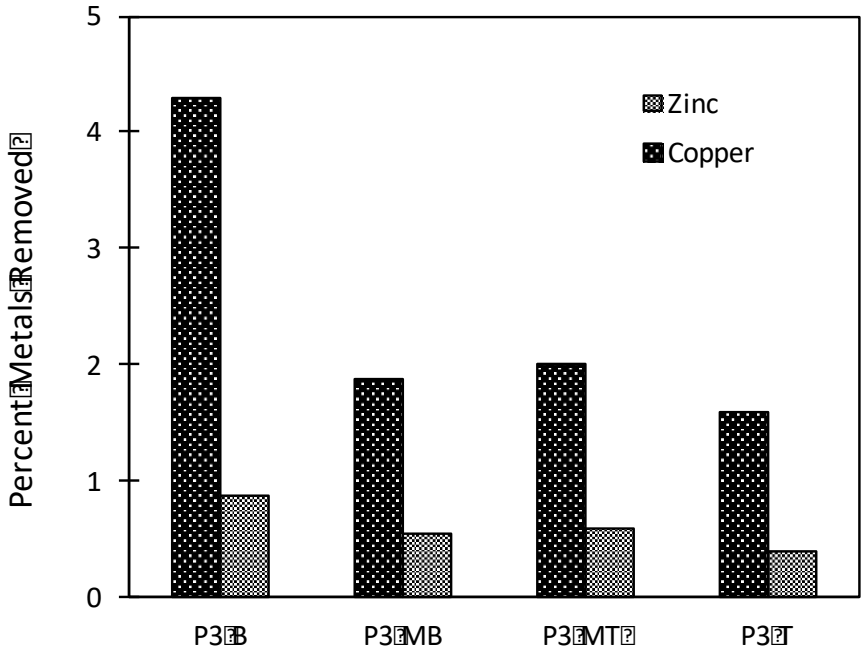

Figure 21. Percent metals removal for quartered sections, bottom (B), mid-bottom (MB), mid-top (MT) and top (T), of Perlite column 3 (P3). Uniform fluid flow through the packed columns was from bottom to top in all experimentation.

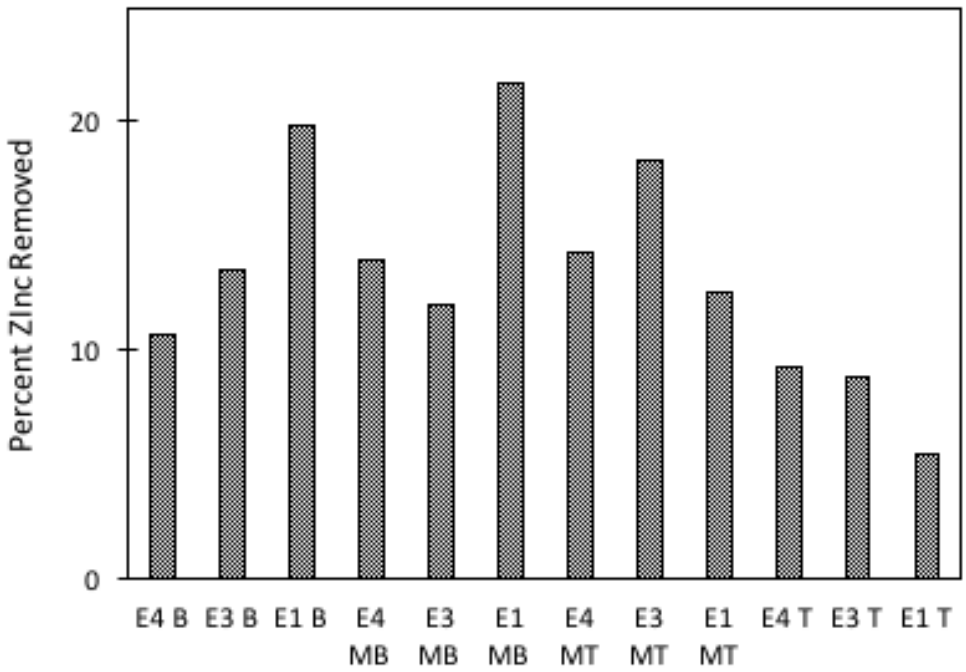

Figure 22. Percent zinc removal for quartered sections, bottom (B), mid-bottom (MB), mid-top (MT) and top (T), of the Earthlite™ columns. Uniform fluid flow through the packed columns was from bottom to top in all experimentation.

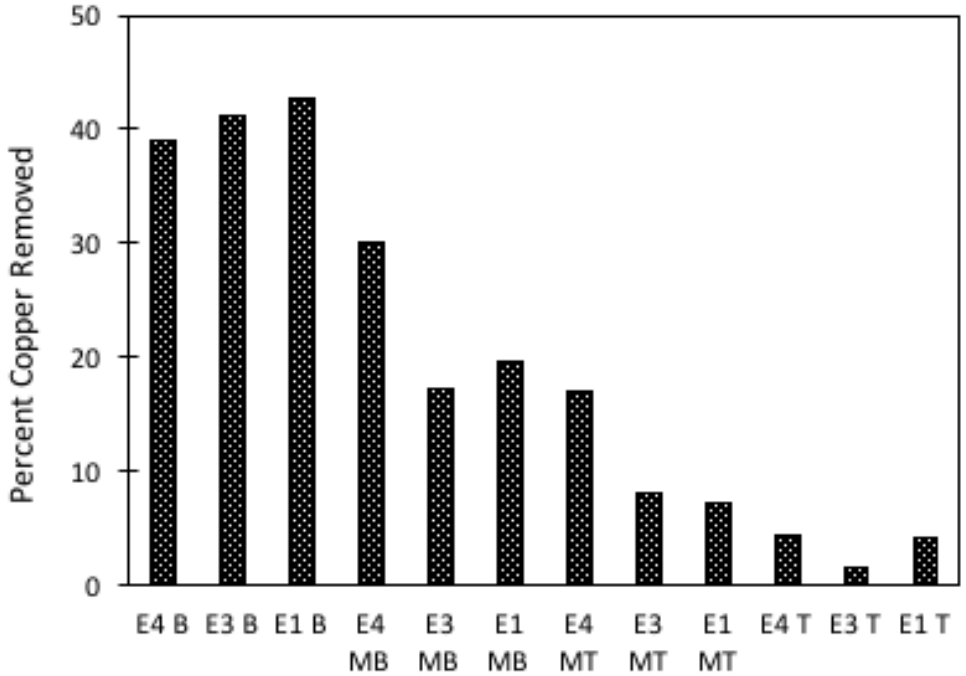

Figure 23. Percent copper removal for quartered sections, bottom (B), mid-bottom (MB), mid-top (MT) and top (T), of the Earthlite™ columns. Uniform fluid flow through the packed columns was from bottom to top in all experimentation.

4.3.2 Earthlite™

Digests conducted for RSSCT done for Earthlite™ (E2) included a grab sample from the entire core and the other Earthlite™ columns (E1, E3 and E4) were quartered with subsamples being pulled from each quarter. The zinc digest removals appeared to correlate with the amount of mass loaded such that as more mass is loaded, the removal increases (Table 4). A similar trend is seen for the copper removal except for E2 which is probably related to the composite core sample. As for percent removal, the bottom three layers have an average zinc removal of 15% and the top layer has an average removal of 8% (Figure 22). All the columns have the lowest percent copper removal in the top layer with a gradual ascension to the highest in the bottom layer and the percent removals are greater than zinc's in the bottom and mid bottom layers (Figure 23). The metals distribution could indicate available zinc sorption capacity remaining in the top column layer only whereas copper appears to have remaining capacity in all but the bottom layer. If more mass had been loaded on the columns, it is possible that the copper would have started to displace zinc as it worked up through the column.

The overall metal's removal estimated from column digests for each column was compared to the removals measured in RSSCT calculated using Equation 12 (Table 4). The Perlite copper digest and RSSCT removal averages are 0.011 ± 0.002 and 0.015 ± 0.002 mg/g, respectively. The Perlite zinc digest removal and RSSCT removal averages are 0.022 ± 0.006 and 0.025 ± 0.002

mg/g, respectively. The Earthlite™ digest removals for zinc are all within the same magnitude and similar to their respective RSSCT removals; the same holds true for the copper removals (Table 4). The similarity and consistency in these values suggest that either technique produces representative medium removal values.

Table 4. Calculated and measured metals removal for Perlite, Earthlite™ and Filter33™ from the arrival wave moment analysis and the column digests, respectively. Pulse width and metals mass loaded were included for referential comparison.

Column	Pulse Width	Cu Mass Loaded, mg	Cu Removal, mg/g	Digest Cu Removal, mg/g	Zn Mass Loaded, mg	Zn Removal, mg/g	Digest Zn Removal, mg/g
E1	220	5.6	0.38	0.29	27	1.69	1.1
E2	400	11	0.65	0.68	45	1.67	1.7
E3	456	11	-	0.49	56	2.66	2.0
E4	430	13	0.69	0.79	66	2.32	2.4
P1	38	1.4	0.011	0.008	6.7	0.028	0.015
P2	10	0.30	0.019	0.012	2.0	0.025	0.034
P3	20	0.39	0.015	0.014	4.0	0.022	0.017
C2	1900	71	-	-	317	9.0	-
C3	1700	64	-	-	276	8.2	-

4.4 Kinetic Batch Studies: Earthlite™

With the discovery of kinetically controlled removal of heavy metals and organic acids in rapid small scale column tests packed with Earthlite™, additional experiments, termed kinetic batch studies, were conducted to further characterize the mechanisms controlling the removal of metals in Earthlite™. Both target metals (with all batch tests conducted using the binary metals

solution) yielded an overall greater maximum removal as initial solution concentration increased (as described by Equation 3) (Figures 24 and 25). These findings agree with kinetic biochar/heavy metal batch tests presented by Kolodynska et al. (2012) and Liu and Zhang (2009). Supporting those results found in column experiments, copper exhibited greater, preferential removal in the presence of Earthlite™ with copper's removal efficiency (Equation 4) measured in batch almost immediately approaching 97-99%, greater than the highly time dependent removal for zinc of approximately 50-90%(Figures 26 and 27). The copper concentration and percent removal increase slightly over the 24 hour test period, achieving nearly instantaneous equilibrium concentrations in the presence of Earthlite™, whereas zinc showed marked kinetically controlled behavior (e.g. significant, nonlinear increases in removal as contact time increases from 5 to 200 min).

Various studies reported in the literature have shown metals uptake to biochar is well described by the pseudo second order (PSO) equation (Equation 5) (e.g. Kolodynska et al. 2012, Liu and Zhang 2009, Chen et al. 2011). The PSO model fits the zinc data well ($R^2 > 0.99$) suggesting that specific sorption is taking place (Table 5). Likewise, average calculated retardation factors (R values in Equation 6) of 4420 and 221 for copper and zinc, respectively, indicate a significant preferential uptake for copper reinforcing the observed competitive effects and apparent instantaneous equilibrium of copper (Table 6).

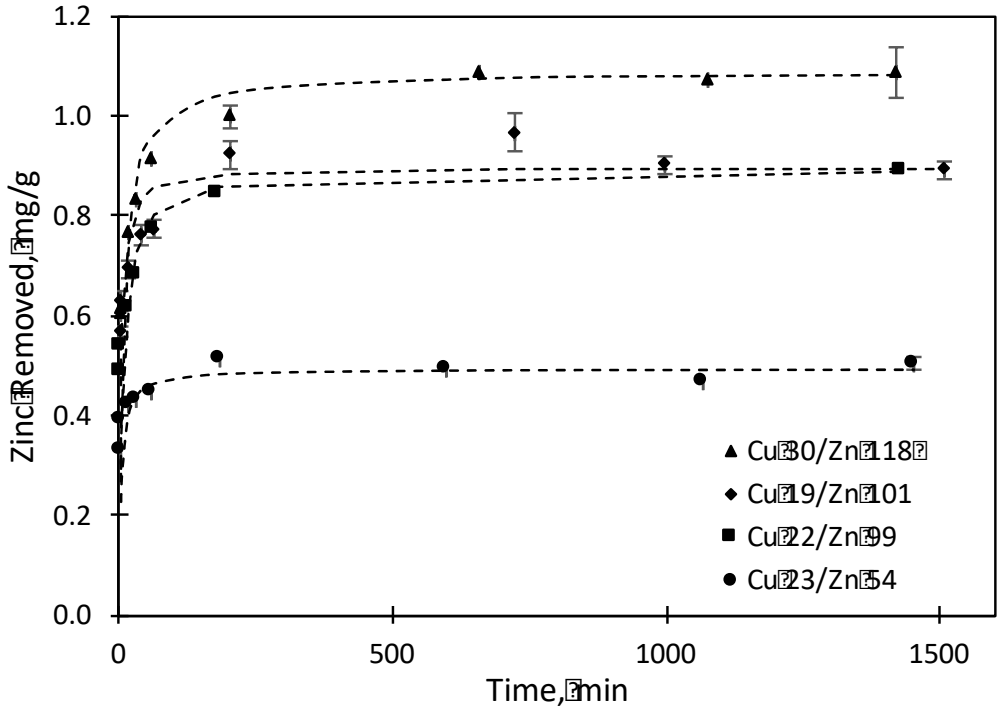

Figure 24. Measured and modeled zinc removal in Earthlite™ kinetic batch tests at various initial concentrations of the binary metals solution.

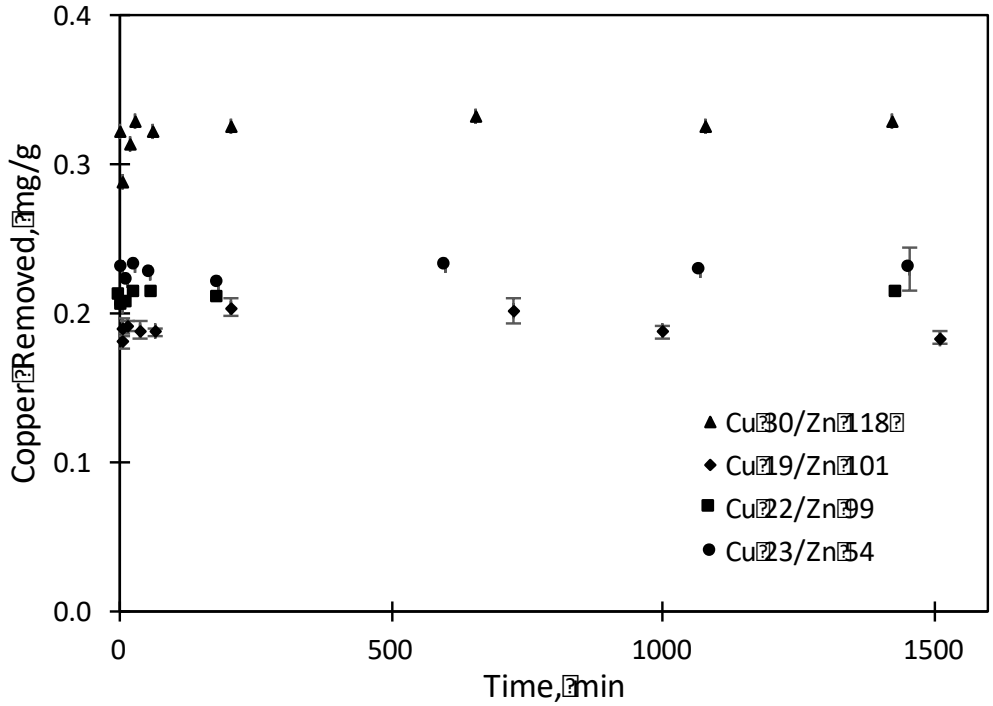

Figure 25. Measured copper removal in Earthlite™ kinetic batch tests at various initial concentrations of the binary metals solution.

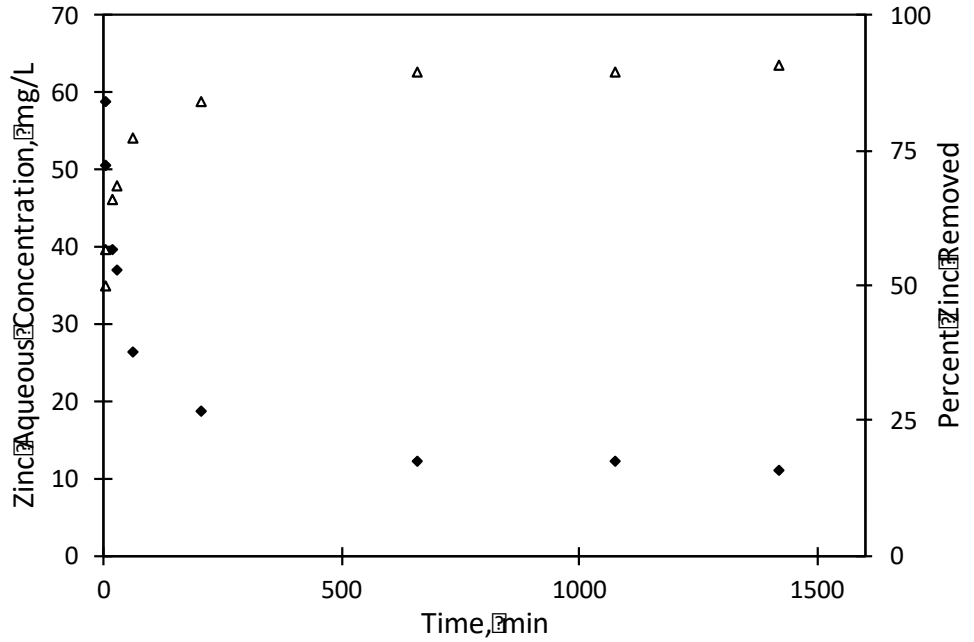

Figure 26. Representative results of zinc aqueous concentration and percent removal in Earthlite™ kinetic batch tests at discrete points over the 24-hour test interval.

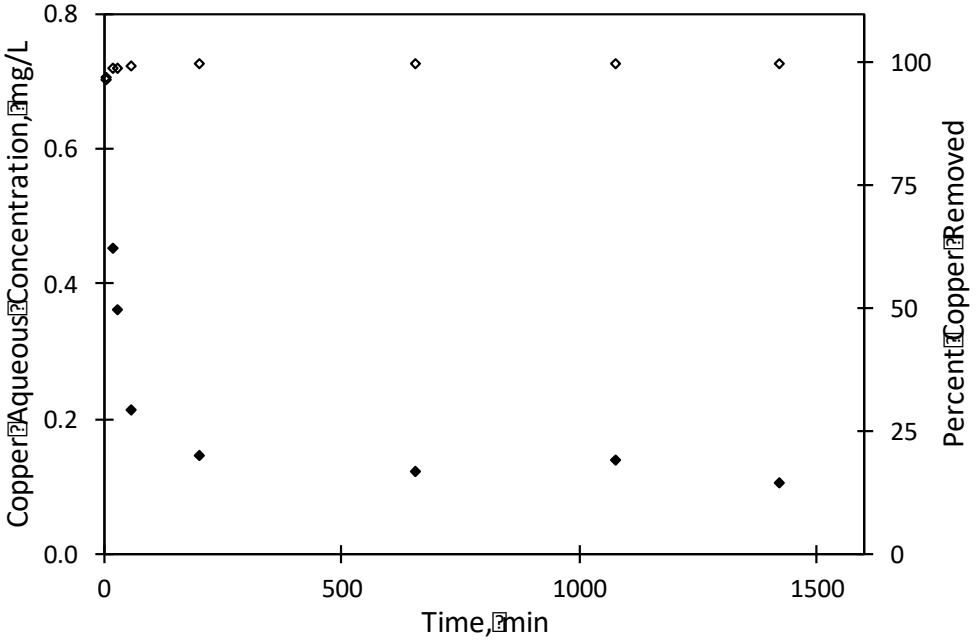

Figure 27. Representative results of copper aqueous concentration and percent removal in Earthlite™ kinetic batch tests at discrete points over the 24-hour test interval.

Representative results of the pH and metals removal show a proportional increase possibly indicative of a proton exchange with the medium such that pH and removal capacity equilibrate at the same rate (Figure 28). It may be interesting to note, the synthetic rainwater medium control held the “equilibrium” pH for the entirety of the batch possibly suggesting that without metal ion competition, H^+ ions immediately and completely interact with the medium through cation ion exchange. Additionally, it appears that an increase in solution pH coincides with a decrease in the solution’s metals concentration as was present in the Earthlite™ columns.

Table 5. Initial zinc concentrations and experimental long-term maximum zinc removal for multiple binary metals Earthlite™ kinetic batch tests with pseudo second order rate constants calculated from zinc removals (mg/g).

C_o, mg/L	$q_{e,\,exp}$, mg/g	q_e, mg/g	k_2, g/(mg min)	R^2
54	0.50	0.49	0.52	0.9979
99	0.89	0.89	0.16	0.9999
101	0.89	0.90	0.37	0.9998
118	1.09	1.09	0.11	0.9998

Table 6. Initial binary metals concentrations for Earthlite™ kinetic batch tests with calculated retardation factors.

Zinc C_o, mg/L	Zinc R	Copper C_o, mg/L	Copper R
54	268	23	3630
99	187	22	4220
101	238	19	3770
118	191	32	6060
Average	221		4420

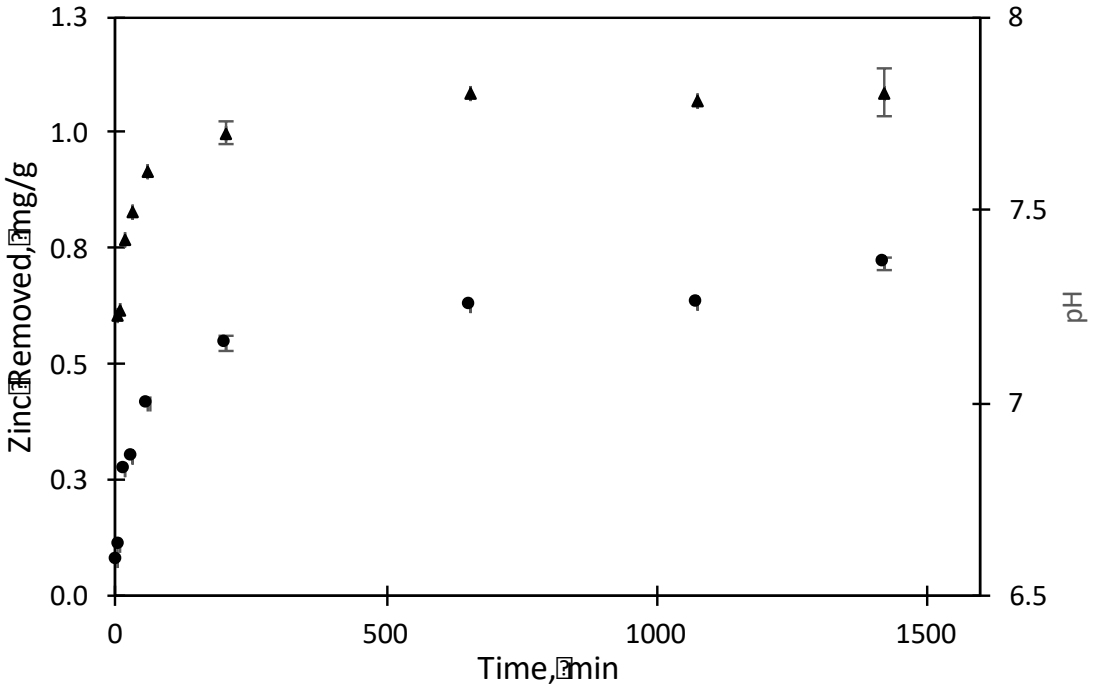

Figure 28. Representative zinc removal and pH from multiple binary metals batch experiments with Earthlite™.

Considering the above results, it is believed that nonspecific and specific sorption mechanisms, as well as competitive effects, are contributing to the metal uptake in Earthlite™. Additionally, since copper is extremely competitive in the aqueous solution (as displayed with the greater percent removal), it is possibly taking up all the nonspecific sites immediately, leaving mostly the specific sorption sites for the zinc. Consequently, there is a rate limited component to the specific sites which could be creating the kinetically controlled PSO uptake of zinc. Similar results were seen by Chen et al. (2011) such that when in a binary solution with Cu(II), Zn(II) displays a decreased removal.

5. CONCLUSION

The results of filtration experiments conducted using various filter media indicate that the transport of metals in Perlite is primarily impacted by nonspecific sorption whereas in Earthlite™ and Filter33™ both nonspecific and specific sorption are present. For all media and experimentation, there was a consistent preferential uptake of copper such that copper displayed delayed arrival and/or greater percent removal than zinc. Moreover, the observed snow plow effects and concentration plateaus in Earthlite™ and Filter33™ RSSCT suggest rate limited ion exchange and specific sorption in addition to ion competition. Supporting those results found in column experiments, copper exhibited greater, preferential removal in the presence of Earthlite™ with copper's removal efficiency measured in batch almost immediately approaching 97-99%, greater than the highly time dependent removal for zinc of approximately 50-90%.

Due to copper's significantly retarded breakthrough in the RSSCT, the following medium removal comparison was based solely on zinc. Perlite had negligible zinc removal, averaging 0.025 ± 0.002 mg/g. The zinc removal obtained for Earthlite™ showed an approach velocity dependent removal efficiency such that as fluid flow decreased Earthlite™ exhibited greater overall removal efficiencies. For example, the zinc removals were 1.60 and 2.60 mg/g at flow rates of 5 and 1 mL/min. This trend is also supported by the retardation factors (130 and 240 at 5 and 1 mL/min) and the results of column digests. Filter33™ displayed the greatest average zinc removal of 8.6 mg/g supported by

its retardation factor of 1100. Earthlite™ and Filter33™ showed organic acid removal capabilities with estimated retardation factors of 2.4 and 5.3, respectively. Further research in necessary to better characterize the observed acid-medium interactions.

When applying these results to expected performance for a mobile media filtration system, removal must be viewed alongside flow rate due to proposed system conditions (i.e. pumping flow rates). Perlite and Filter33™ could handle the upper flow rate of 10 mL/min (the lab scale equivalent of the proposed field scale flow); Earthlite™'s maximum flow was 5 mL/min. Considering flow, measured copper and zinc removals and proposed TSS removal, Perlite and Filter33™ could possibly work well in series (i.e. a treatment train approach to stormwater management) wherein a Perlite filter removes TSS before the stormwater is introduced to Filter33™, potentially prolonging the life and efficiency of the system. Future studies are warranted to investigate the feasibility of the proposed series configuration using synthetic stormwater. In addition, system operators need to be aware of the possibility of concentration spikes after a system flow interruption and recirculation of at least the first bed volume is advised. Moreover, the Filter33™ elution results indicate that medium regeneration (i.e. desorption) potential is correlated to the previously loaded mass thus delays/lapses in medium maintenance could result in lengthy or incomplete regeneration. In all, this research indicates that test parameters (i.e. pH, competitive ions solutions, empty bed contact time, flow rate) based on the

natural environment and field scale operation can greatly impact removal efficiency in filter media.

REFERENCES

Alkan, M., and Doğan, M. (2001). Adsorption of copper(II) onto perlite. *Journal of Colloid and Interface Science*, *243*(2), 280–291. https://doi.org/10.1006/jcis.2001.7796

American Public Heath Association (APHA) (2012). Standard Methods for the Examination of Water and Wastewater, 22nd edn. Washington, DC: American Public Heath Association.

ASTM. (2001). *Sieve Analysis of Fine and Coarse Aggregates* (C136). West Conshohocken, PA: ASTM International.

ASTM. (2010). *Classification of Soild for Engineering Purposes (Unified Soil Classification System)* (D2487). West Conshohocken, PA: ASTM International.

Baldwin, D. H., Tatara, C. P., and Scholz, N. L. (2011). Copper-induced olfactory toxicity in salmon and steelhead: Extrapolation across species and rearing environments. *Aquatic Toxicology*, *101*(1), 295–297. https://doi.org/10.1016/j.aquatox.2010.08.011

Barrett, M. E. (2005). Performance comparison of structural stormwater best management practices. *Water Environment Research*, *77*(1), 78–86. https://doi.org/10.2175/106143005x41654

Bay, S., Jones, B. H., Schiff, K., and Washburn, L. (2003). Water quality impacts of stormwater discharges to Santa Monica Bay. *Marine Environmental Research*, *56*(1–2), 205–223. https://doi.org/10.1016/S0141-1136(02)00331-8

Bilotta, G. S., and Brazier, R. E. (2008). Understanding the influence of suspended solids on water quality and aquatic biota. *Water Research*, *42*(12), 2849–2861. https://doi.org/10.1016/j.watres.2008.03.018

Brookes, A. (1986). Response of aquatic vegetation to sedimentation downstream from river channelisation works in England and Wales. *Biological Conservation*, *38*(4), 351–367. https://doi.org/10.1016/0006-3207(86)90060-1

Bureau of Environmental Services (BES). (2004). *Stormwater Solutions Handbook*. Portland. Retrieved from www.nature.org/healthyair

Bureau of Environmental Services (BES). (2016). *City of Portland Stormwater*

Management Manual. https://doi.org/10.1016/B978-1-85617-567-8.50011-1

Caetano, M., Valderrama, C., Farran, A., and Cortina, J. L. (2009). Phenol removal from aqueous solution by adsorption and ion exchange mechanisms onto polymeric resins. *Journal of Colloid and Interface Science*, *338*(2), 402–409. https://doi.org/10.1016/j.jcis.2009.06.062

Charters, F. J., Cochrane, T. A., and O'Sullivan, A. D. (2016). Untreated runoff quality from roof and road surfaces in a low intensity rainfall climate. *Science of the Total Environment*, *550*, 265–272. https://doi.org/10.1016/j.scitotenv.2016.01.093

Chen, X., Chen, G., Chen, L., Chen, Y., Lehmann, J., McBride, M. B., and Hay, A. G. (2011). Adsorption of copper and zinc by biochars produced from pyrolysis of hardwood and corn straw in aqueous solution. *Bioresource Technology*, *102*(19), 8877–8884. https://doi.org/10.1016/j.biortech.2011.06.078

Clarus Water Solutions. (2015). *Products.* Retrieved May 24, 2018, from http://claruswatersolutions.com/products.htm/

CONTECH® Stormwater Solutions Inc. (2001). *Product Evaluation: Silt loam TSS removal efficiency of a stormwater BMP*. CONTECH® Stormwater Solutions Inc.: Portland OR.

CONTECH® Stormwater Solutions Inc. (2015). *StormFilter Configuration Guide*. CONTECH® Stormwater Solutions Inc.: Portland OR.

Davis, A. P., Shokouhian, M., and Ni, S. (2001). Loading estimates of lead, copper, cadmium, and zinc in urban runoff from specific sources. *Chemosphere*, *44*(5), 997–1009. https://doi.org/10.1016/S0045-6535(00)00561-0

Gary, Miles and Kleber, Markus. (2015). *University Research Test Results.* Retrieved from http://earth-lite.com/rain/stormwater-results/university-research-information/.

Ghassabzadeh, H., Mohadespour, A., Torab-Mostaedi, M., Zaheri, P., Maragheh, M. G., and Taheri, H. (2010). Adsorption of Ag, Cu and Hg from aqueous solutions using expanded perlite. *Journal of Hazardous Materials*, *177*(1–3), 950–955. https://doi.org/10.1016/j.jhazmat.2010.01.010

Gironás, J., Adriasola, J. M., and Fernández, B. (2008). Experimental Analysis and Modeling of a Stormwater Perlite Filter. *Water Environment Research*,

80(6), 524–539. https://doi.org/10.2175/193864708X267432

Gu, B., Mehlhorn, T. L., Liang, L., and McCarthy, J. F. (1996). Competitive adsorption, displacement, and transport of organic matter on iron oxide: II. Displacement and transport. *Geochimica et Cosmochimica Acta*, *60*(16), 2977–2992. https://doi.org/10.1016/0016-7037(96)00157-3

Harsh, J. (2005). Amorphous Materials. *Encyclopedia of Soils in the Environment* (pp: 64-71). Elsevier. https://doi.org/10.1016/B0-12-348530-4/00207-1

Helfferich, F., and Plesset, M. S. (1958). Ion exchange kinetics. A nonlinear diffusion problem. *The Journal of Chemical Physics*, *28*(3), 418–424. https://doi.org/10.1063/1.1744149

Huber, M., Welker, A., and Helmreich, B. (2016). Critical review of heavy metal pollution of traffic area runoff: Occurrence, influencing factors, and partitioning. *Science of the Total Environment*, *541*, 895–919. https://doi.org/10.1016/j.scitotenv.2015.09.033

Janvion, P., Motellier, S., and Pitsch, H. (1995). Ion-exchange mechanisms of some transition metals on a mixed.pdf, *715*, 105–115.

Johnson, D. (2005). POLLUTANTS | Persistent Organic (POPs). In *Encyclopedia of Soils in the Environment* (pp. 264–271). Elsevier. https://doi.org/10.1016/B0-12-348530-4/00560-9

Kayhanian, M., Stransky, C., Bay, S., Lau, S. L., and Stenstrom, M. K. (2008). Toxicity of urban highway runoff with respect to storm duration. *Science of the Total Environment*, *389*(2–3), 386–406. https://doi.org/10.1016/j.scitotenv.2007.08.052

Kinerson, R. S., Mattice, J. S., and Stine, J. F. (1996). The Metals Translator: Guidance For Calculating A Total Recoverable Permit Limit From A Dissolved Criterion. *United States Environmetal Protection Agency: Office of Water*, (June), 1–67. https://doi.org/EPA 823-B-96-007

Kołodyńska, D., Wnetrzak, R., Leahy, J. J., Hayes, M. H. B., Kwapiński, W., and Hubicki, Z. (2012). Kinetic and adsorptive characterization of biochar in metal ions removal. *Chemical Engineering Journal*, *197*, 295–305. https://doi.org/10.1016/j.cej.2012.05.025

Kumar, S., and Jain, S. (2013). History, introduction, and kinetics of ion exchange materials. *Journal of Chemistry*, *2013*. https://doi.org/10.1155/2013/957647

Liu, Z., and Zhang, F. S. (2009). Removal of lead from water using biochars prepared from hydrothermal liquefaction of biomass. *Journal of Hazardous Materials*, *167*(1–3), 933–939. https://doi.org/10.1016/j.jhazmat.2009.01.085

Mathialagan, T., & Viraraghavan, T. (2002). Adsorption of cadmium from aqueous solutions by perlite. *Hazardous Materials*, *94*, 291–303. https://doi.org/10.1081/SS-120016698

Minerals Education Coalition (MEC). Minerals Database: Perlite. Minerals Education Coalition. Retrieved on from https://mineralseducationcoalition.org/minerals-database/perlite/

Morel, Francois M.M. and Hering, Janet G. (1993) *Principles and Applications of Aquatic Chemistry.* New York, NY: John Wiley and Sons, Inc.

Muralikrishna, I. V., and Manickam, V. (2017). Industrial Wastewater Treatment Technologies, Recycling, and Reuse. In *Environmental Management* (pp. 295–336). Elsevier. https://doi.org/10.1016/B978-0-12-811989-1.00013-0

Nason, J. A., Sprick, M. S., and Bloomquist, D. J. (2012). Determination of copper speciation in highway stormwater runoff using competitive ligand exchange - Adsorptive cathodic stripping voltammetry. *Water Research*, *46*(17), 5788–5798. https://doi.org/10.1016/j.watres.2012.08.008

New Jersey Department of Environmental Protection (NJCAT). (2007). *NJCAT Technology Verification Stormwater Management Stormfilter Contech Stormwater Soltuions Inc.* Retrieved from http://www.imbriumsystems.com/Portals/0/documents/sc/testing/NJCAT Verification Stormceptor OSR 2007.pdf

Oregon Department of Environmental Quality (ODEQ). (2003). *Biofilters for Stormwater Discharge Pollution Removal*. Retrieved from http://www.oregon.gov/deq/FilterPermitsDocs/biofiltersV2.pdf

Oregon Department of Environmental Quality (ODEQ). (2017). *Portland Harbor : Catch Basins*.

Pankow, James F. (1991) *Aquatic Chemistry Concepts.* Beaverton, OR: Lewis Publishers.

Peña-Icart, M., Villanueva Tagle, M. E., Alonso-Hernández, C., Rodríguez Hernández, J., Behar, M., and Pomares Alfonso, M. S. (2011). Comparative study of digestion methods EPA 3050B (HNO3-H2O2-HCl) and ISO 11466.3

(aqua regia) for Cu, Ni and Pb contamination assessment in marine sediments. *Marine Environmental Research*, *72*(1–2), 60–66. https://doi.org/10.1016/j.marenvres.2011.05.005

Ribaudo, M. O. (1986). Consideration of Offsite Impacts in Targeting Soil Conservation Programs. *Land Economics*, *62*(4), 402–411.

Sandahl, J. F., Baldwin, D. H., Jenkins, J. J., and Scholz, N. L. (2007). A sensory system at the interface between urban stormwater runoff and salmon survival. *Environmental Science and Technology*, *41*(8), 2998–3004. https://doi.org/10.1021/es062287r

Sari, A., Tuzen, M., Citak, D., and Soylak, M. (2007). Adsorption characteristics of Cu(II) and Pb(II) onto expanded perlite from aqueous solution. *Journal of Hazardous Materials*, *148*(1–2), 387–394. https://doi.org/10.1016/j.jhazmat.2007.02.052

Selim, H. M., Buchter, B., Hinz, C., and Ma, L. (1992). Modeling the Transport and Retention of Cadmium in Soils: Multireaction and Multicomponent Approaches. *Soil Sci, Soc. Am. J*, *56*(January), 1004–1015. https://doi.org/10.2136/sssaj1992.03615995005600040002x

Silber, A., Bar-Yosef, B., Suryano, S., & Levkovitch, I. (2012). Zinc adsorption by perlite: Effects of pH, ionic strength, temperature, and pre-use as growth substrate. *Geoderma*, *170*(3), 159–167. https://doi.org/10.1016/j.geoderma.2011.11.028

Soil Science Society of America (2018). *Rain Gardens and Bioswales.* Retrieved from https://www.soils.org/discover-soils/soils-in-the-city/green-infrastructure/important-terms/rain-gardens-bioswales

Starr, J. L., and Parlange, J.-Y. 1979. Dispersion in Soil Columns: The Snow Plow Effect1. *Soil Sci, Soc. Am. J*. 43:448-450. doi:10.2136/sssaj1979.03615995004300030005x

Sunmark Environmental. *Earthlite Stormwater Filter Media.* Retrieved from http://earth-lite.com/rain/

Swayampakula, K., Boddu, V. M., Nadavala, S. K., & Abburi, K. (2009). Competitive adsorption of Cu (II), Co (II) and Ni (II) from their binary and tertiary aqueous solutions using chitosan-coated perlite beads as biosorbent. *Journal of Hazardous Materials*, *170*(2–3), 680–689. https://doi.org/10.1016/j.jhazmat.2009.05.106

United States Environmental Protection Agency. (2009). *Industrial Stormwater Monitoring and Sampling Guide*.

United States Environmental Protection Agency. (2017). *Polluted Runoff : Nonpoint Source Pollution*. Retrieved from https://www.epa.gov/nps/what-nonpoint-source

United States Environmental Protection Agency. (2018a). *Impaired Waters and Stormwater*. Retrieved from https://www.epa.gov/tmdl/impaired-waters-and-stormwater

United States Environmental Protection Agency. (2018b). *National Pollutant Discharge Elimination System (NPDES)*. Retrieved from https://www.epa.gov/npdes/npdes-stormwater-program

Vaaramaa, K., and Lehto, J. (2003). Removal of metals and anions from drinking water by ion exchange. *Desalination*, *155*(2), 157–170. https://doi.org/10.1016/S0011-9164(03)00293-5

APPENDIX A. Solids Analysis

Table 1. Total Suspended Solids (TSS) for TriMet Merlo stormwater samples. B2 had %difference > 4% and was omitted.

Sample	initial mass filter+boat (g)	final mass filter+boat (g) 1/22/17	Volume (ml)	mass TSS (g)	mass TSS (mg)	TSS (mg/L)= mass TSS (mg) /vol (mL)*1000	Average TSS (mg/L)
blank	2.1764	2.1757	60	-0.0007			
A1	2.1986	2.2103	35	0.0117	12	334	
A2	2.2619	2.2709	30	0.0090	9	300	
A3	2.2551	2.2661	32	0.0110	11	344	326
B1	2.2016	2.2076	63	0.0060	6	95	
B3	2.2126	2.2174	50	0.0048	5	96	96
C1	2.1986	2.2016	97	0.0030	3	31	
C2	2.2877	2.2905	93	0.0028	3	30	
C3	2.2521	2.2554	114	0.0033	3	29	30

Table 2. Total Solids (TS) for TriMet Merlo stormwater samples. A2 and C1 had %difference > 4% and were omitted.

Sample	initial mass filter+boat (g)	final mass filter+boat (g) 1/22/17	Volume (ml)	mass TSS (g)	mass TSS (mg)	TSS (mg/L)= mass TSS (mg) /vol (mL)*1000	Average TSS (mg/L)
blank	49.5336	49.5292	61	-0.0044			
A1	49.9475	49.9846	103	0.0371	37	360	
A3	49.2657	49.306	114	0.0403	40	354	357
B1	49.2366	49.2564	155	0.0198	20	128	
B2	50.0729	50.0938	160	0.0209	21	131	
B3	49.4699	49.4881	145	0.0182	18	126	128
C2	47.9114	47.9681	471	0.0567	57	120	
C3	60.6605	60.7155	450	0.055	55	122	121

Table 3. Total Dissolved Solids (TDS) for TriMet Merlo stormwater samples.

Sample	initial mass filter+boat (g)	final mass filter+boat (g) 1/22/17	Volume (ml)	mass TSS (g)	mass TSS (mg)	TSS (mg/L)= mass TSS (mg) /vol (mL)*1000	Average TSS (mg/L)
blank	49.2274	49.2216	61	61	0	ND	ND
A1			35				
A2			30				
A3	49.2971	49.2945	32	97	0	ND	ND
B1			63				
B2			44				
B3	61.1724	61.1815	50	157	0	9	58
C1			97				
C2			93				
C3	48.4375	48.462	114	304	0	25	81

APPENDIX B. Particle Size Analysis

Table 4. Earthlite™ particle size analysis.

Sieve Number	Mass Total (pan+media) (g)	Mass media (g)	% on Sieve	Cumulative %	Particle Size (mm)	Percent Passing
1/4	375.26	38.28	17.7	17.72	6.30	82.28
4	412.67	37.41	17.3	35.05	4.75	64.95
6	452.71	40.04	18.5	53.59	3.35	46.41
10	493.02	40.31	18.7	72.25	2	27.75
40	546.97	53.95	25.0	97.23	0.42	2.77
200	552.95	5.98	2.8	100.00	0.075	0.00
>200	552.95	0.00	0.0	100.00	<0.075	0.00
	Total Mass	215.97				

Table 5. Perlite particle size analysis.

Sieve Number	Mass Total (pan+media) (g)	Mass media (g)	% on Sieve	Cumulative %	Particle Size (mm)	Percent Passing
1/4	336.93	0.00	0.0	0.00	6.30	100.00
4	337.03	0.10	0.2	0.21	4.75	99.79
6	342.7	5.77	11.9	12.12	3.35	87.88
10	370.23	33.30	68.7	80.85	2	19.15
40	344.04	7.11	14.7	95.52	0.42	4.48
200	337.92	0.99	2.0	97.56	0.075	2.44
>200	338.11	1.18	2.4	100.00	<0.075	0.00
	Total Mass	48.45				

Table 6. Filter33™ particle size analysis.

Sieve Number		Mass media (g)	% on Sieve	Cumulative %	Particle Size (mm)	Percent Passing
1/4			0.0	0.00	6.30	100.00
4			0.0	0.00	4.75	100.00
40		48.69	18.3	18.29	0.43	81.71
60		156.95	59.0	77.25	0.25	22.75
100		59.57	22.4	99.62	0.15	0.38
200		1.00	0.4	100.00	0.075	0.00
>200			0.0	100.00	<0.075	0.00
	Total Mass	266.21				